An-Najah National University

Faculty of Graduate Studies

Electrochromic Properties of Electrodeposited (NiO) Thin Films: Optimization of Synthesis Parameters

By

Mustafa Naeem Husain Waked

Supervisor

Dr. Iyad Saadeddin

Co-Supervisor

Dr. Mohammed Suleiman Shtaya

This Thesis is Submitted in Partial Fulfillment of Requirements for the Degree of Master of Physics, Faculty of Graduate Studies, An-Najah National University- Nablus, Palestine

2017

Electrochromic Properties of Electrodeposited (NiO) Thin Films: Optimization of synthesis Parameters

By

Mustafa Naeem Husain Waked

This thesis was defended successfully on /10/2017, and approved by:

Defense Committee Members	**Signature**
– Dr. Iyad Saadeddin / Supervisor	**……**
– Dr. Mohammed Suleiman Shtaya / Co-Supervisor	**…….**
– Prof. Atef Qasrawi / External Examiner	**...……..**
– Prof. Ismail Khalil Warad/ Internal Examiner	**...……..**

Dedication

To my parents especially Mother who took care of me after my father (may God have mercy upon him)

To my dear brother "Husain"(may God have mercy upon him)

To my twin brother "Muath"

To my dear sisters "Ahlam and Hadeel"

To Mohammad Anwar Hamdan (Abu-Anwar) &Ahmad Zaki yahya (Abu-Alaa) who helped me in my educational process

To my family who interested me

To those who are looking forward for more knowledge…

Acknowledgments

The First and final Thanks to Almighty Allah After that, I would dedicate deep thanks and grateful to my supervisor Dr. Iyad Saadeddin who was as a beacon by continuous followings, helpful effort and encouragement. I do not also forget my Co- Supervisor Dr. Mohammed Suleiman. Who was forming distinguished team with my supervisor.

The members working in physics and chemistry departments especially, Prof. Atef Qasrawi (Arab American University, Department of physics), Mr. Mohammad Bahjat (An-Najah National University, Department of physics), and Mr. Nafeth Zakrea (An-Najah National University, Department of chemistry), they Deserve my thanks and appreciation due to continuous supporting and kind dealing and help me to take necessary tests and measurements to accomplish this work. Special thanks to my brother "Muath Waked" for helping me in some translation.

Finally, I would take this chance to express on deep appreciation and grateful to my family (My Parents, sisters, brother, Uncles, Aunts and Mr. Zaki mohammad waked (Abu Asama)).

Who stand behind me to pass this degree

Mustafa

الإقرار

أنا الموقع أدناه مقدم الرسالة التي تحمل عنوان

Electrochromic Properties of Electrodeposited (NiO) Thin Films: Optimization of synthesis Parameters

أقر بأن ما اشتملت عليه هذه الرسالة انما هو نتاج جهدي الخاص،باستثناء ما تمت الاشارة اليه حيثما ورد ،وأن هذه الرسالة ككل من أو جزء منها لم يقدم من قبل لنيل أي درجة أو بحث علمي أو بحثي لدى أية مؤسسة تعليمية أو بحثية أخرى.

Declaration

The work provided in this thesis, unless otherwise referenced, is there searcher's own work, and has not been submitted elsewhere for any other degree or qualification.

Student's name: **اسم الطالب:**

Signature: **التوقيع:**

Date: **التاريخ:**

List of Contents

Dedication III

Acknowledgments IV

Declaration V

List of Contents VI

List of Tables IX

List of Figures X

Abstract XIV

Chapter One 1

Introduction and theoretical background 1

Chapter One 2

Introduction and theoretical background 2

1.1 Objectives 2

1.2 Why nickel oxide (NiO) based thin films? 2

1.3 Previous studies 3

1.4 Chromism 6

1.5 Electrochromism 7

1.5.1 Electrochromic device (ECDs) and their applications 7

1.6 Back ground on nickel compound 10

1.6.1 Nickel oxide compound 10

1.6.2 Nickel hydroxide $Ni(OH)_2$ 10

1.6.3 Nickel oxihydroxide NiOOH 11

1.6.4 Mechanism of coloration 12

1.7 Deposition techniques of NiO–based thin films 13

1.7.1 Physical techniques 13

1.7.2 Chemical techniques 13

1.7.3 Elecrochemical deposition (ECD) 14

Chapter Two 16

Experimental Work 16

2.1 Materials and film preparation 17

2.1.1 Chemicals and solvents 17

2.1.2 Substrate cleaning process 17

2.1.3 Preparation of NiO based films 19

2.2 Measurements 21

2.2.1 Cyclic voltammetry (CV) 21

2.2.2 Chronoamperometry (CA) 23

2.2.3 Transmittance 23

2.3 Instruments 24

Chapter Three 29

Results and Discussion 29

3.1 Effect of cleaning process : adhesion and uniformity of Ni-based films…..... 30

3.2 Electrodeposition potential optimization for Ni-based electrochromic thin films. 39

3.2.1 $Ni(OH)_2$ electrochromic films 39

3.2.2 NiO electrochromic films..... 53

3.3 Optimization of nickel nitrate molar concentration for Ni-based thin films electrodeposition. 62

3.3.1 $Ni(OH)_2$ electrochromic films..... 62

3.3.2 Molar concentration effect on NiO electrochromic films..... 67

3.3.2.2. Molar concentration effect on NiO optical parameters 71

3.4 General conclusions 80

References 83

الملخص ..... ب

List of Tables

Table (2.1): Schematic shows weights of the molar concentrations used. . 19

Table (3.1): Deduced and calculated electrochromic parameters for films before annealing ($Ni(OH)_2$) deposited using different deposition potentials (mV). 45

Table (3.2): Calculated thickness for $Ni(OH)_2$ films deposited using different deposition potentials. 49

Table (3.3): The optical band gap for $Ni(OH)_2$ films deposited at different potentials. 52

Table (3.4): Deduced and calculated electrochromic parameters for films after annealing (NiO) deposited using different deposition potentials (mV). 56

Table (3.5): Calculated thickness for NiO films prepared using different deposition potentials. 60

Table 3.6: The optical band gap for $Ni(OH)_2$ films deposited at different potentials. 61

Table (3.9): Calculated thickness for NiO films prepared using molar concentration of $Ni(NO_3)_2.6H_2O$. 73

Table (3.10): The optical band gap for NiO films deposited at different potentials. 75

Table (3.11): Deduced and calculated electrochromic parameters for cycle number 2, 200, 400 of NiO thin film prepared at optimum conditions (-700 mV deposition potential, 1M $Ni(NO_3)_2.6H_2O$, and annealed at 300 ºC). 80

List of Figures

Figure (1.1): Schematic diagram for ECD showing its different layers. 8

Figure (1.2): Schematic shows states of electrochromic device operation... 9

Figure (1.3): Schematic shows picture format in EC mirror and normal mirror. 9

Figure (1.4.a): Shows β-$Ni(OH)_2$ phase [45]. 10

Figure (1.4.b): Shows α-$Ni(OH)_2$ phase [45]. 11

Figure (1.6): Bode scheme for NiO electrode oxidation reduction reaction [42]. 12

Figure (1.7): Experimental arrangement for film growth in ECD. 15

Figure (2.1): Procedure of NiO-based films deposition by electrodeposition technique. 20

Figure (2.2): Cycling voltammetry waveform. 21

Figure (2.3): A schematic shows one compartment three electrodes electrochemical cell. 22

Figure (2.4): Potential wave form for chronoamperometry. 23

Figure (2.5): The photos shows PGZ402 universal potentiostate instrument. 24

Figure (2.6): Shows shimadzu UV-3101PC UV-VIS-NIR scanning spectrophotometer device. 25

Figure (2.7): : Elma ultrasonic cleaner. 26

Figure (2.8): Bifa laboratory furnaces. 26

Figure (2.9): The schematic shows Rikago miniflex 600 diffractometer... 28

Figure (3.1): Normal photos for different prepared films at different cleaning process: a) as deposited films (B: before annealing) and b) films after post annealing at 300 °C for one hour under air (A: after annealing)..... 32

Figure (3.4): Microscope photos (×100 magnification) for films after post annealing at 300 °C for one hour under air with different cleaning processes after annealing (A). 35

Fig. (3.5): Microscope photos (×400 magnification) for films after post annealing at 300 °C for one hour under air with different cleaning processes..... 36

Figure (3.6): CA curves during twenty cycles for $Ni(OH)_2$ films deposited at deferent deposition potentials. Potential cycled between -650 mV and 650 mV versus Ag/AgCl reference electrode in 0.5 M KOH electrolyte. 40

Figure (3.7): The shematic explains how to find Q_a, Q_c, t_b and t_c values. .. 41

Figure (3.8): The schematic shows how to find T_b and T_c also t_b and t_c. ... 42

Figure (3.10): Linear sweep voltammogram for $Ni(NO_3)_2.6H_2O$ solution done at 50 mV/s versus Ag/AgCl reference electrode. 47

Figure (3.11): Transparency spectra for $Ni(OH)_2$ deposited at different deposition potentials. The inset shows the fringes for film deposited at -600 mV..... 48

Figure (3.12): The plot of $(\alpha E)^2$ as a function of E $Ni(OH)_2$ deposited using different deposition potentials. 51

Figure (3.13): CA curves during twenty cycles for NiO films deposited at deferent deposition potentials. Potential cycled between -650 mV and 650 mV versus Ag/AgCl reference electrode in 0.5 M KOH electrolyte. 54

Figure (3.14): Optical transmittance change at 630 nm wave length during CA for NiO thin films deposited at different potentials. 55

Figure (3.15): Cyclic voltammetry measurments for Ni-based thin films: a) NiO thin film annealing at 300 ˚C (A- after annealing) and b) as deposited film $Ni(OH)_2$ (B: before annealing). 57

Figure (3.16): Transparency spectra for NiO films prepared at different deposition potentials. 59

Figure (3.17): The plot of $(\alpha E)^2$ as a function of E for NiO films prepared using different deposition potentials. 61

Figure (3.18): Twenty CA cycles $Ni(OH)_2$ thin films prepared using different molar concentrations of $Ni(NO_3)_2.6H_2O$ potential cycled between -650 mV and 650 mV versus Ag/AgCl reference electrode in 0.5M KOH. 64

Figure (3.21): Optical transmittance change at 630 nm wave length during CA for NiO thin films deposited using different concentrations of $Ni(NO_3)_2.6H_2O$..... 69

Figure (3.22): Transparency spectra for NiO films prepared from different $Ni(NO_3)_2.6H_2O$ concentrations. 72

Figure (3.25): CA curve for cycles 2, 200, and 400 of electrochromic NiO film prepared at optimal conditions (1 M $Ni(NO_3)_2.6H_2O$, -700 mV deposition potential, and annealed at 300 ºC). 78

Figure (3.26): Optical transmittance change at 630 nm wave length of NiO thin films with voltages -700 mV after annealing at 300 ˚C for one houre under air at molar concentration 1M. 79

XIV

Electrochromic Properties of Electrodeposited (NiO) Thin Films: Optimization of Synthesis Parameters

By
Mustafa Naeem Husain Waked
Supervisors
Dr. Iyad Saadeddin
Dr. Mohammad Suleiman Shtaya

Abstract

NiO thin films were prepared by electrodeposition technique onto fluorine-doped tin oxide-coated glass substrates (FTO glass). For these films, a comparative study for the influence of various cleaning processes, deposited voltages, and molar concentrations on adhesion, homogeneity, electrochromic properties, structural properties, and optical properties were studied. Adhesion and homogeneity properties were studied using intermediate magnification microscope (×100 and ×400). Electrochromic (coloration efficiency, reversibility, switching time and stability) properties was investigated using chronoamperometry, cyclic voltametry and transparency during chronoamperometry. Transparency spectrum in the range between (200-1000 nm), was also used to investigate some optical parameters (transparency, film thickness and optical energy band gap). Best adhesion and homogeneous properties were observed, for films prepared using dish washing liquid soap followed by successive immersion of substrates into sonicated isopropanol, aceton and ethanol. These films were soacked in diluted HCL, before finally rinsed with deionized water and dried at 100 ^{o}C. Highest electrochromic and optical properties was obtained for NiO films prepared on pre-cleaned FTO/Glass substrate, prepared at -

700 mV, molar concentration of 1 M $Ni(NO_3)_2.6H_2O$, and annealed at 300 ^oC under air. This film shows a poly crystallite structure with grain size of 12 nm as confirmed by XRD measurements.

Chapter One

Introduction and theoretical background

Chapter One

Introduction and theoretical background

1.1 Objectives

The objectives of this study are to deposite homogeneous, good adhesive and high electrochromic performance nickel oxide (NiO) thin films by electrodeposition technique.

Following parameters are to be optimized to have films with above intended properties:

a- Different substrate cleaning processes.

b- Deposition of 1M nickel oxide (NiO) thin films at different voltage (-1000, -800, -700, -600 and -500 mV).

c- Different molar concentration of nickel oxide (1M, 0.8M, 0.5M, 0.3M and 0.1M) at the same voltage -0.7V.

1.2 Why nickel oxide (NiO) based thin films?

Nickel oxide is ranked in second class after tungsten oxide as one of popular electrochromic materials. In addition, it could be used as a complementary electrode with WO_3. Because of its high electrochromic efficiency, Nickel oxide films have many features like cyclic reversibility (highly stable), durability and coloration. It is useful for smart windows technology and it has a good dynamic range (low potential operation range) [1].

Nickel oxide is anti ferromagnatic material, and a metal –deficient p-type semiconductor with a band gap 3.6 eV. The nickel oxide is used in many

applications like electrochromic display devices, catalysts, gas sensors and fuel cells [2-8].

Nickel oxide films can be fabricated by many deposition techniques; thermal evaporation, chemical vapor deposition, spray pyrolysis, sol-gel, chemical solution deposition, electrochemical deposition and sputtering [9-18]. All of these methods give different features based on the application of interest. Therefore, there are many efforts to have films with chemical and physical properties as required.

In this thesis the electrodeposition method is employed to preparation nickel oxide films because firstly this process is easy to operate and its needs simple equipment. Secondly, the control of the deposition rate is simple by controlling the current or voltage.

1.3 Previous studies

Usha and his group studied the electrochromic properties of NiO thin film that was prepared by radio frequency (rf) magnetron sputtering technique. They found that the coloration efficiency, reversibility and optical modulation were 235 cm^2/C, 64% and 58%, respectively. They also found the coloration and bleaching time were 1.25 and 1.1 second, respectively [19].

Velevska and his team prepared (NiO) thin film by chemical bath deposition. They studied the electrochromic properties for NiO thin film. They found that the coloration efficiency at 670 nm was 40.6 m^2/C and the response time for coloring and bleaching were 4.00 s and 2.65 s, respectively [20].

Brown and his group prepared the NiO thin films on indium tin oxide by electrodeposition technique. They studied the electrochromic properties of NiO thin films that were fabricated using two deposition process; the first process by using the shorter potential limits and the second process by using wider potential limits. The calculated coloration efficiency for two deposition processes were 49 cm^2/C and 10 cm^2/C, respectively [21].

Patel and his group deposited the nickel oxide (NiO) thin films on glass and ITO glass substrates at room temperature by e-beam evaporation. The coloration efficiency was 22 cm^2/C and 19 cm^2/C at 650 nm and 1000 nm wave lengths, respectively. They found the energy band gap and transmittance were 3.78 eV and 55% [22].

Patil and his group deposited nickel oxide thin films (NiO) on glass substrate by sol gel spin coating method. They studied the morphology, structural, electrical, and optical properties of nickel oxide thin films at various temperatures from 400 °C to 700 °C for one hour under air. They found that the NiO has nanocrystalline cubic structure and grain size of 40 – 60 nm. They also observed the electrical conductivity was increased from 10^{-4} to 10^{-2} Ω.cm when annealing temperature was increasing from 400 °C to 700 °C. The optical properties were decreased from 3.86 eV to 3.47 eV with increasing temperature from 400 °C to 700 °C [23].

Sonavane and his team prepared nickel oxide on FTO glass by electrode position method in one step deposition for 20, 30, 40 and 50 minutes. They studied the effect of thickness of the film on the optical, morphological, structural and electrochromic properties. They found that the optical

transmittance decreased when the film thickness was increasing. They also observed that the films deposited for 20 minutes have the maximum coloration efficiency (107 cm^2/C) and electrochemical stability up to 104 color/bleach cycles [24].

Akaltun and Cayir studied the effect of film thickness on morphological, optical and structural properties when synthesis nickel oxide thin films at room temperature on glass substrate by successive ionic layer adsorption and reaction (SILAR) method. They found that when increasing film thickness the resistivity changed between 4.1 and 802.1 Ω.cm also the surface and crystalline properties were improved. The values of energy gap were reduced from 3.71 eV to 3.67 eV depending on thickness of the film [25].

Sen and his team studied electrical and optical properties of nickel oxide (NiO) doped with various concentrations of zinc (0% to 0.5% to 4%) by sol gel spin coating method. They found when increasing at 4% dopant concentration, the resistivity and absorption peak was increased also at lower dopant concentration. The nickel oxide doped with zinc was a suitable hole conductor for the device applications of solar cell [26].

Vigneshkumar and his group studied the structural and optical properties of nickel oxide (NiO) thin film prepared by spray pyrolysis method. They found the reflectance and transmittance of the nickel oxide thin film were 7% and 83% respectively at 550 nm wave length. Also they found that the direct band gap was 3.2 eV [27].

Guziewicz and his team studied the optical and electrical properties of nickel oxide thin film with various temperatures from 300 °C to 900 °C by

RF magnetron. They found that nickel oxide thin film depended on the temperature of substrate and amount of oxygen through sputtering. They found that when deposited the nickel oxide thin film at room temperature in the absence of the oxygen, the resistivity was 65 Ω.cm and the transmittance was near 50% in the visible rang. On the other hand, when oxygen quantity increased in deposition gas mixture the conductivity was higher but the transmittance was decrease below 6%. Moreover, the conductivity was lower when the films were deposited at temperatures above 500 °C [28].

Gowthami and his group prepared nickel oxide thin films by spray method. They studied the optical properties of nickel oxide at various temperatures from 350 ˚C to 450 ˚C. They found the optical transmittance was decreased, and the optical band gap was also decreased with increasing substrate temperature [29].

Saleh prepared nickel oxide thin films on quartz substrates by rapid thermal oxidation technique at 850 ˚C and various oxidation time. He studied the structural properties of nickel oxide thin film, he found that when increased the oxidation time the grain size was increased. Also he found that all of the films prepared at various oxidation times display cubic structure [30].

1.4 Chromism

Chromism is a process that has changes in the compounds color by many external stimuli [31], and it is classified according to these stimuli as follows: thermochromism (by heat), photochromism (by light),

solvatochromism (by solvent polarity), piezochromism (by pressure) and electrochromism (by electric current), …..etc.

In our study, electrochromism will be choosed because this chromism type constitutes with work topic.

1.5 Electrochromism

1.5.1 Electrochromic device (ECDs) and their applications

1.5.1.1 Design and operation of ECDs

The electrochromic devices change the optical properties like reflectance, absorption and transmission by the control with the charge (insertion or extraction) [32, 33]. The ECDs are used in many applications such as electrochromic display devices, mirrors and electrochromic windows because the obvious property (change the optical property). Also ECD consists from five layers which are two transparent conducting layers (FTO or ITO) and electrolyte (ion conductor) that separates between two electrochromic thin film one of them cathodic coloration and the other anodic coloration [34, 35].

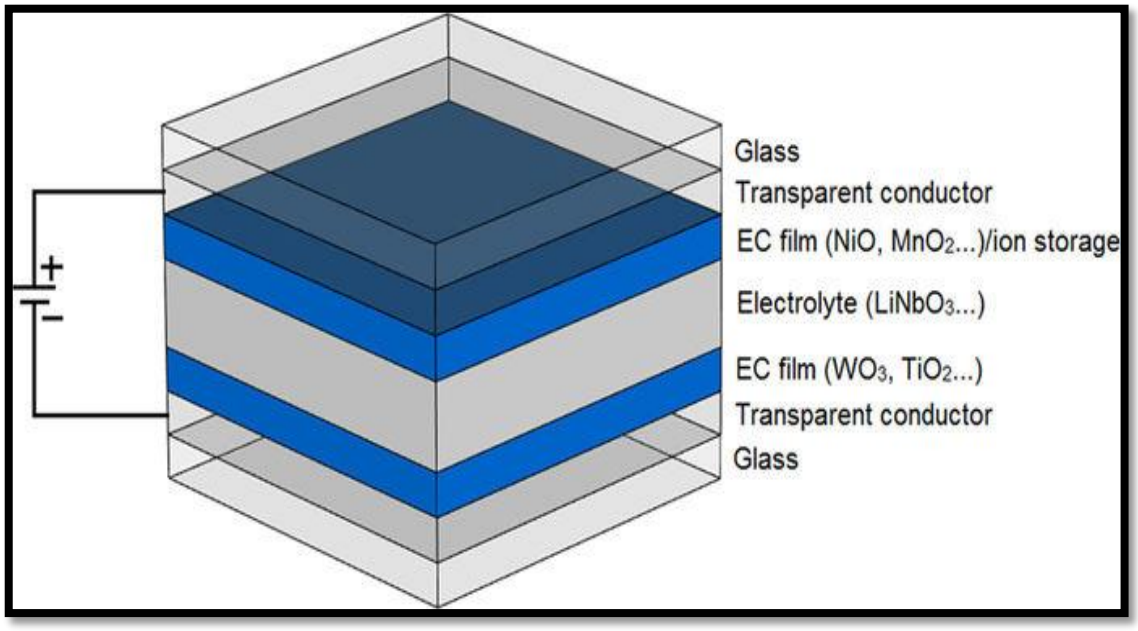


Figure (1.1): Schematic diagram for ECD showing its different layers.

1.5.1.2 Application of ECDs as electrochromic windows (ECWs)

There are many examples of electrochromic devices like filters, rear-view mirrors, EC windows, display and helmets [36]. EC windows and electrochromic mirrors will be stated below.

a) Electrochromic windows

The electrochromic windows control the amount of solar energy and visible light that are passing through the windows by two states or two modes as shown in figure (1.2), where they are bleached state (off state) and colored state (on state). In bleached state part of solar energy and visible light are passing through ECW inside the room and the window looks transparent, as known ITO or FTO films reflect infrared radiation. In color state the amount of visible light and solar energy passing through the ECW is reflected and the window looks dark.

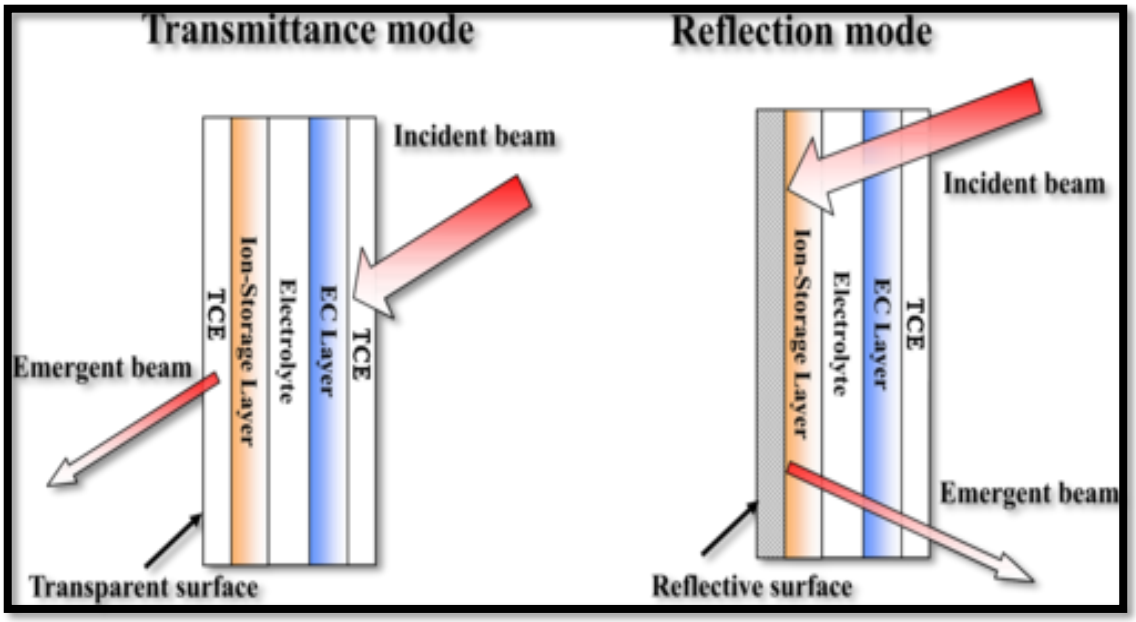


Figure (1.2): Schematic shows states of electrochromic device operation.

b) Electrochromic mirror

As shown in figure (1.3), the EC mirror controls the amount of flashing light that is emitted from vehicles at night through regulating the amount of reflections, this feature makes the driver see without discomfort.



Figure (1.3): Schematic shows picture format in EC mirror and normal mirror.

1.6 Back ground on nickel compound

1.6.1 Nickel oxide compound

Nickel is a transition metal since its one of group VIII elements in periodic table. The transition elements have many features such as ductility, malleability, and conductivity for heat and electricity. They also have valence electrons that are existing in more than one shell and used to join the transition elements with other elements. This often gives many common oxidation states. Useful alloys are appeared when nickel is added to metals, this strength, hardness, and corrosion resistance would be increased [37].

1.6.2 Nickel hydroxide $Ni(OH)_2$

Nickel hydroxide consists of two known phases that are β-$Ni(OH)_2$ phase and the α-$Ni(OH)_2$ phase. The β structure is layered structure and each layer has an hexagonal plan configuration of Ni(II) ions with an oxygen octahedral coordinate. The distance between layers 4.6 Å as shown in figure (1.4.a) [38-44].

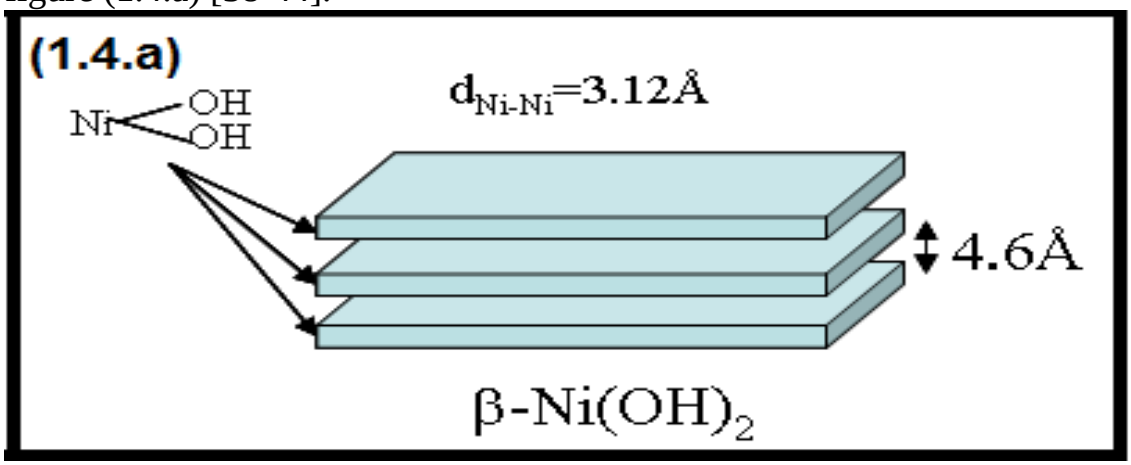


Figure (1.4.a): Shows β-$Ni(OH)_2$ phase [45].

The hydration of the β-$Ni(OH)_2$ phase is α-$Ni(OH)_2$ phase where the molecules of water are intercalated among $Ni(OH)_2$ layers. This leads to large distance between layers was 8.0 Å as shown in figure (1.4.b) [39-42].

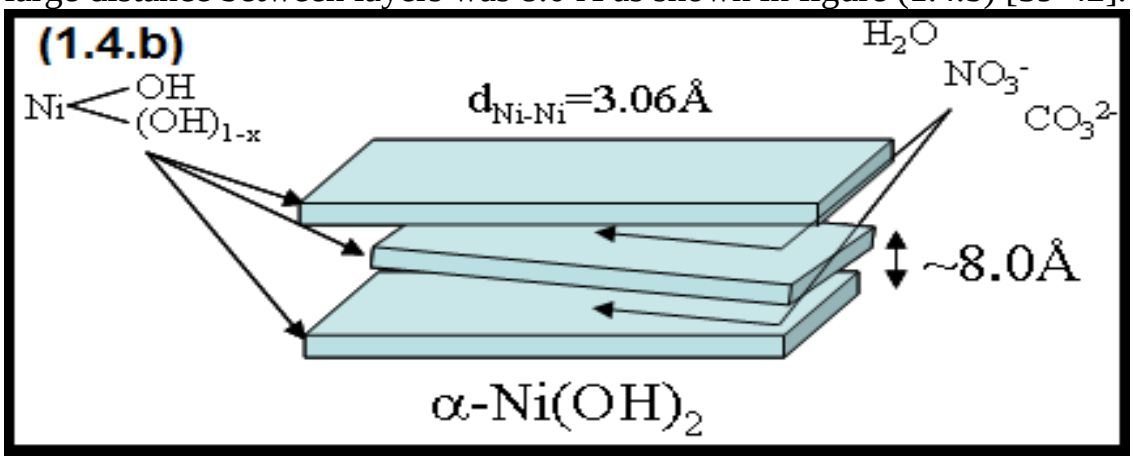


Figure (1.4.b): Shows α-$Ni(OH)_2$ phase [45].

1.6.3 Nickel oxihydroxide NiOOH

Nickel oxihydroxide consists of two phases γ-NiOOH and β-NiOOH. The γ-NiOOH is generally represented by the formula $A_xH_y(H_2O)_z.NiO_2$ and have the oxidation state range between 3 and 3.75. Both phases of NiOOH: β-NiOOH and γ-NiOOH look like brown thin film and have inter-sheet distance 4.7 Å for β-NiOOH phase and 7.0 Å for γ-NiOOH phase [38-41].

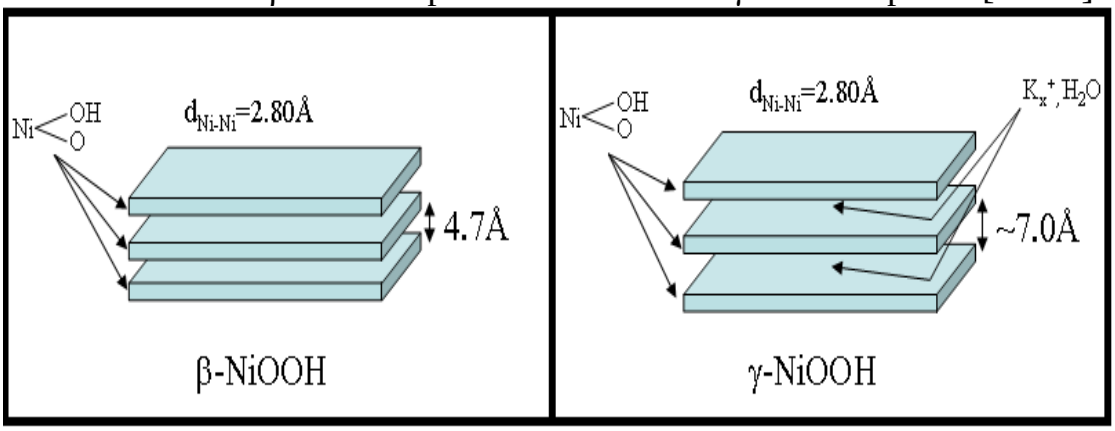


Figure (1.5): Shows γ-NiOOH and β-NiOOH phases [45].

1.6.4 Mechanism of coloration

From mechanism of coloration, chemical and electrochromic properties could be investigated for Ni-based thin films through immersing Ni-based thin film in aqueous electrolyte like (KOH). When immersing NiO particles in KOH electrolyte. The surface of NiO is converted into nickel hydroxide $Ni(OH)_2$. This was done through redox (reduction/oxidation) reaction. Bode et al. proposed this reaction through scheme that shows hydrated NiO electrode immersed in KOH electrolyte [42].

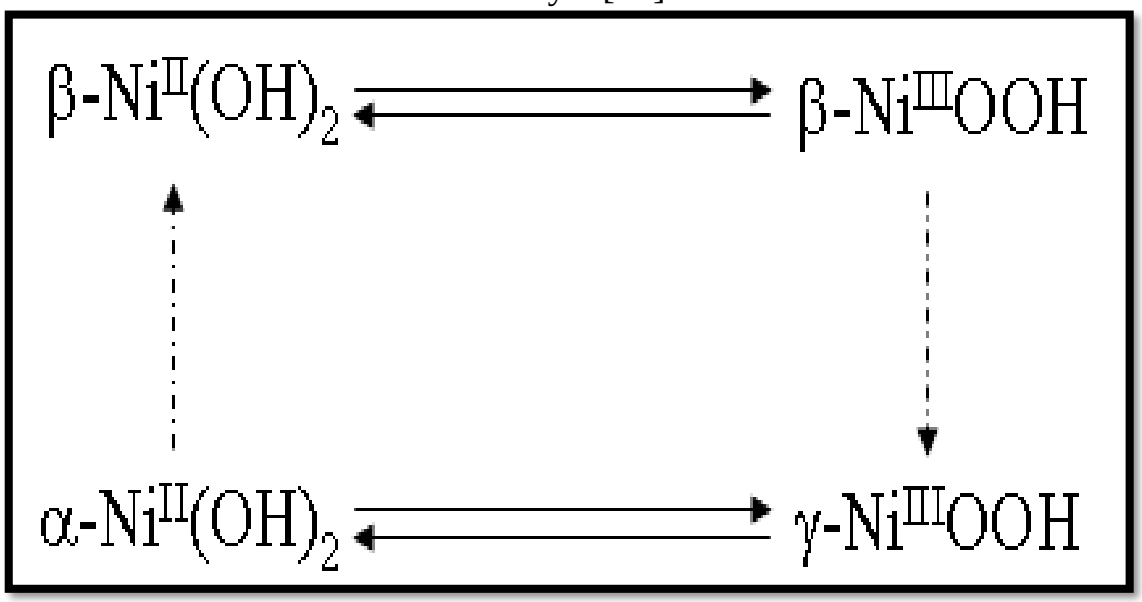


Figure (1.6): Bode scheme for NiO electrode oxidation reduction reaction [42].

The Bode scheme shows transition between Ni(II) and Ni(III), it also displays two redox reactions are β-$Ni(OH)_2$/ β-NiOOH (β^{II}/β^{III}) and α-$Ni(OH)_2$/ γ-NiOOH (α/γ) [40]. In the redox reaction, 1.3 electrons are transferred when deals with transformation α/γ [46-47].

In the electrochromic mechanism, there are three major reactions (1.1, 1.2 and 1.3) when NiO thin films are studied in aqueous electrolyte. $Ni(OH)_2$

and NiO are transparent but NiOOH is colored in the form of thin film [40, 48, 49-52].

$$Ni(OH)_2 \leftrightarrow NiOOH + H^+ + e^- \quad (1.1)$$

$$Ni(OH)_2 + OH^- \leftrightarrow NiOOH + H_2O + e^- \quad (1.2)$$

$$NiO + OH^- \leftrightarrow NiOOH + e^- \quad (1.3)$$

1.7 Deposition techniques of NiO–based thin films

There are many techniques in order to prepare electrochromic NiO thin films. The main method is classified into physical, chemical, and electrochemical techniques.

1.7.1 Physical techniques

Physical deposition techniques are characterized by a process in which the material goes from a condensed phase to a vapor phase and then back to a thin film condensed phase. It includes sputtering [53-56], electron beam evaporation [57], pulse laser deposition [58, 59], and etc.

1.7.2 Chemical techniques

In chemical deposition techniques, a fluid precursor undergoes a chemical change at a solid surface, leaving a solid layer. some chemical methods for thin film deposition are chemical bath deposition [60], dip coating in a sol-gel [61-63], spin coating of a sol-gel solution [64], and etc.

1.7.3 Elecrochemical deposition (ECD)

In our work, we have used electrochemical technique to deposit our Ni-based electrochromic films. The main features of the electrochemical technique are:

Very low cost of manufacturing.

Large area manufacturing.

Compatibility with substrates variety.

Figure (1.7) shows a three-electrode electrochemical experimental arrangement for CdS thin film preparation on ITO/Glass substrate (adopted as an example). It included a solution containing distilled water, chemical materials and HCl in order to control PH value. The temperature of solution was kept under constant stirring during deposition and a constant temperature oil bath [65]. The platinum plate and pre-cleaned substrate that has dimensions 1×4 cm^2 were held by holders and partially immersed in the chemical solution. The system was well closed under a continuous nitrogen flow. By an applied potential of a DC stripping, deposition was occurred.

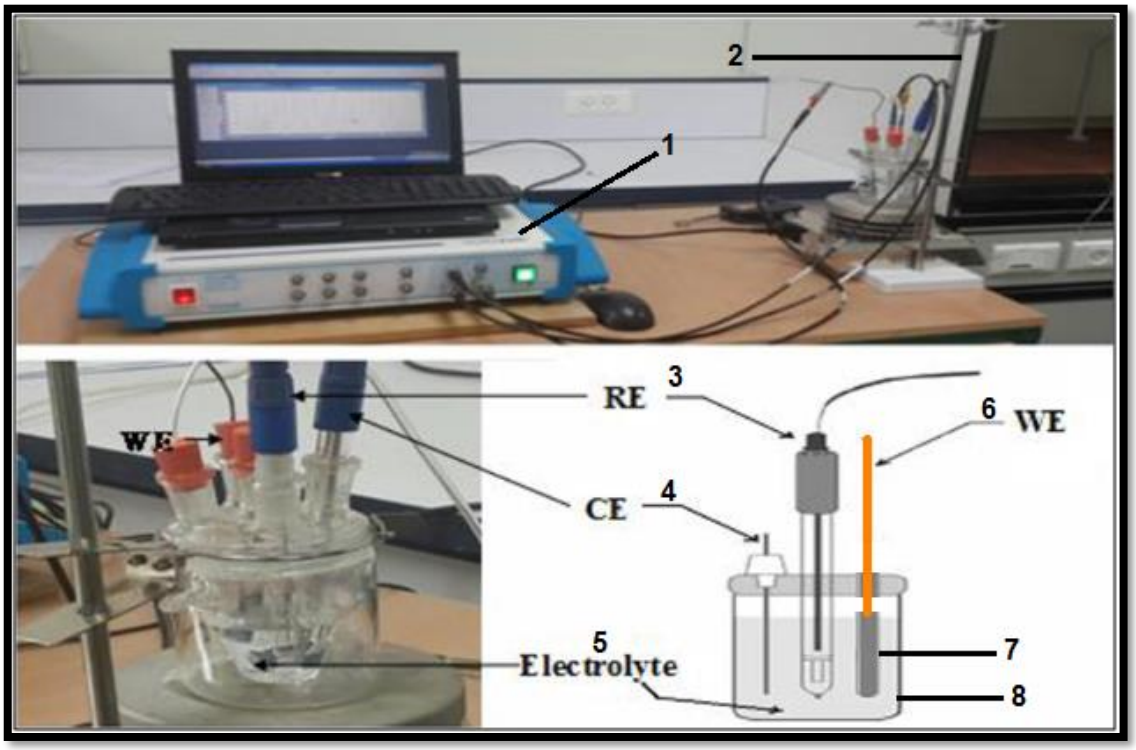


Figure (1.7): Experimental arrangement for film growth in ECD.

1. Potentiostate; 2. Clamp stand; 3. Reference electrode (AgCl/Ag); 4. Counter Electrode (platinum); 5. Electrolyte; 6. Working electrode; 7. FTO/Glass substrate; 8. Beaker (60 ml).

Chapter Two

Experimental Work

Chapter Two

Experimental Work

2.1 Materials and film preparation

2.1.1 Chemicals and solvents

In its pure form, materials are purchased from different companies:

1- Nickel (II) nitrate hexahydrate [$Ni(NO_3)_2.6H_2O$] was purchased from Aldrich.

2- Potassium hydroxide (KOH) is from Frutarom.

3- Other materials like isopropanol, methanol, ethanol, hydrofluoric acid (HF) and hydrochloric acid (HCl) are self-packing locally.

4- Highly transparent and conductive in the visible florine-doped tin dioxide on glass (FTO/ glass) samples were used as substrates.

2.1.2 Substrate cleaning process

FTO/glass substrates that have dimensions of 5×1 cm^2 were prepared in order to deposit NiO-depending on electrochromic films. It is necessary to use pre-cleaned substrates. In order to study the effect of cleaning method on film uniformity and adhesion, the substrates were cleaning using different cleaning methods:

a- First method (M_1):

1-Cleaning (FTO/glass) substrate with dish washing liquid (Fairy dish washing liquid 2.5 ml in 50 ml tap water) to remove any attachments or dust.

2-Washing substrate by tap water, after that washing with deionized water to remove fairy liquid.

3-Drying (FTO/glass) substrate with pressed air and immersing it in HCl for two minutes to remove any un-cleaned attaches.

4-Washing with deionized water and drying with pressed air.

5-Dryingthe substrate at 100 °C for five minutes.

b- Second method (M_2):

Same cleaning procedure as M_1, but we change step 1 in M_1 by dipping the substrate in sonicator for ten minutes.

c- Third method (M_3):

Same cleaning steps as (M_1), but we add a new step (after step 2 in M_1), which is immersing air dried substrate in ethanol under sonication for ten min. using ultrasound sonicator.

d- Fourth method (M_4):

Same as M_3 cleaning method, but ethanol is replaced by a ceton in the sonication step.

e- Fifth method (M_5):

Again as M_3 cleaning process, but ethanol is now replaced by isopropanol in the ultra-sonication step.

f- Sixth method (M_6):

Also, this cleaning process is same as M_3, but in ultra-sonication step, we have immersed the substrate in the three solutions (ethanol, a ceton, and

isopropanol) successively. Each solution was kept under sonication for ten minutes.

g- Seventh method (M_7):

Same cleaning process as M_6. However, HCL is replaced by HF before finally washed and dried.

2.1.3 Preparation of NiO based films

Electrochromic (NiO) thin film was prepared using electrodeposition technique followed by annealing at 300 ˚C for one hour under air, $Ni(NO_3)_2.6H_2O$ with appropriate molar concentration (0.1M, 0.3M, 0.5M, 0.8M and 1M), was added to 25 ml of distilled water and stirred by a magnet for 20 minutes. This gives a transparent green color.

Table (2.1): Schematic shows weights of the molar concentrations used.

Molar Concentration	Weight (gm)
0.1 M	0.73
0.3 M	2.18
0.5 M	3.63
0.8 M	5.81
1.0 M	7.27

The prepared electrolyte solutions were deposited on the previously cleaned (FTO/glass) substrate using electrodeposition technique.



Figure (2.1): Procedure of NiO-based films deposition by electrodeposition technique.

The steps of electrodeposition operation for (NiO) –based film is appeared in figure (2.1) and abbreviated as follows:

1. Placing the cleaned (FTO/glass) substrate in to electrolyte solution and connect it to the working electrode.
2. Depositing the film on the substrate. this is done by filling the electrodeposition parameters in the potentiostate software before running the experiment. we have used chronocalorimetry experiment to deposit our film on the substrate. The parameters filled are the deposition potential and the time duration, which can be limited by charge magnitude.
3. Drying the slides under air for one day.
4. Annealing at 300 °C into the oven under air for one hour to get (NiO) film.
5. Electrodeposition of Ni-based films was done for under different deposition potentials (-500, -600, -700, -800, -1000 mV) and different $Ni(NO_3)_2.6H_2O$

concentrations (0.1, 0.3, 0.5, 0.8, 1.0 M) in the solution to optimize best parameters for Ni-based electrochromic films.

2.2 Measurements

2.2.1 Cyclic voltammetry (CV)

Cycling voltammetry is an electrochemical technique and performed using cycling the working electrode potential and measuring the current that develops in an electrochemical cell.

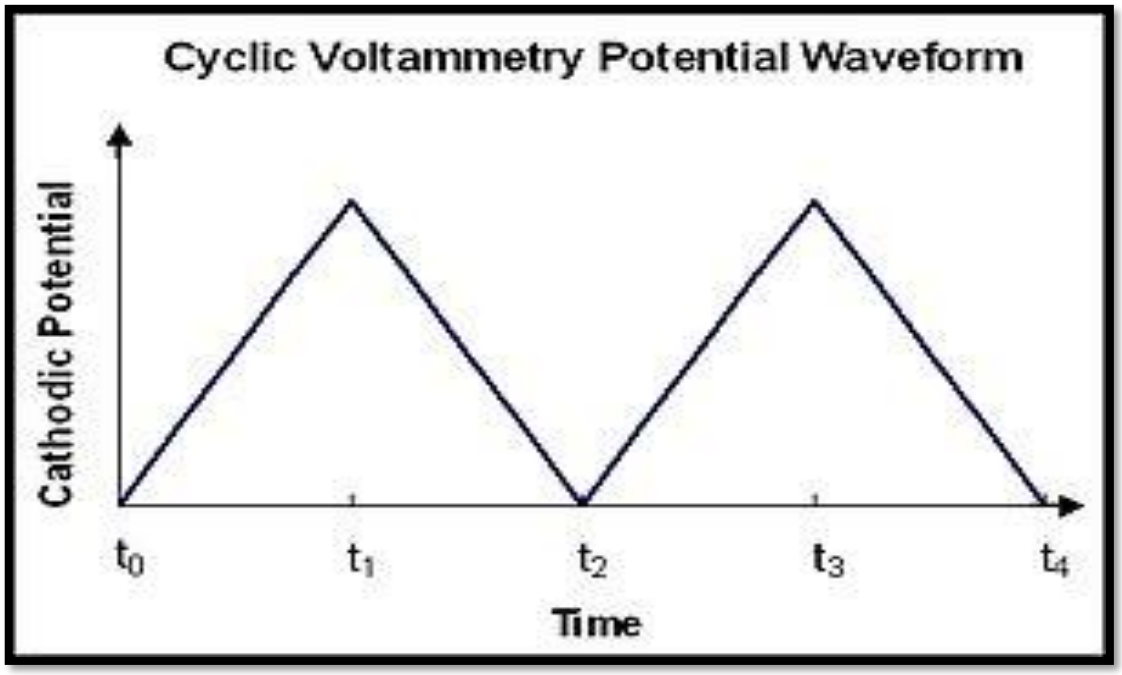


Figure (2.2): Cycling voltammetry waveform.

Figure (2.3), shows three electrodes electrochemical cell used to do the cyclic voltammetry tests. It usually contains aqueous solution as an electrolyte. The NiO electrochemical films precipitated on FTO/Glass substrate were involved in the cell as working electrode (WE). Silver

chloride/silver (AgCl/Ag) was participated as reference electrode (RE) in the cell and as a counter electrode (CE), the platinum was involved.

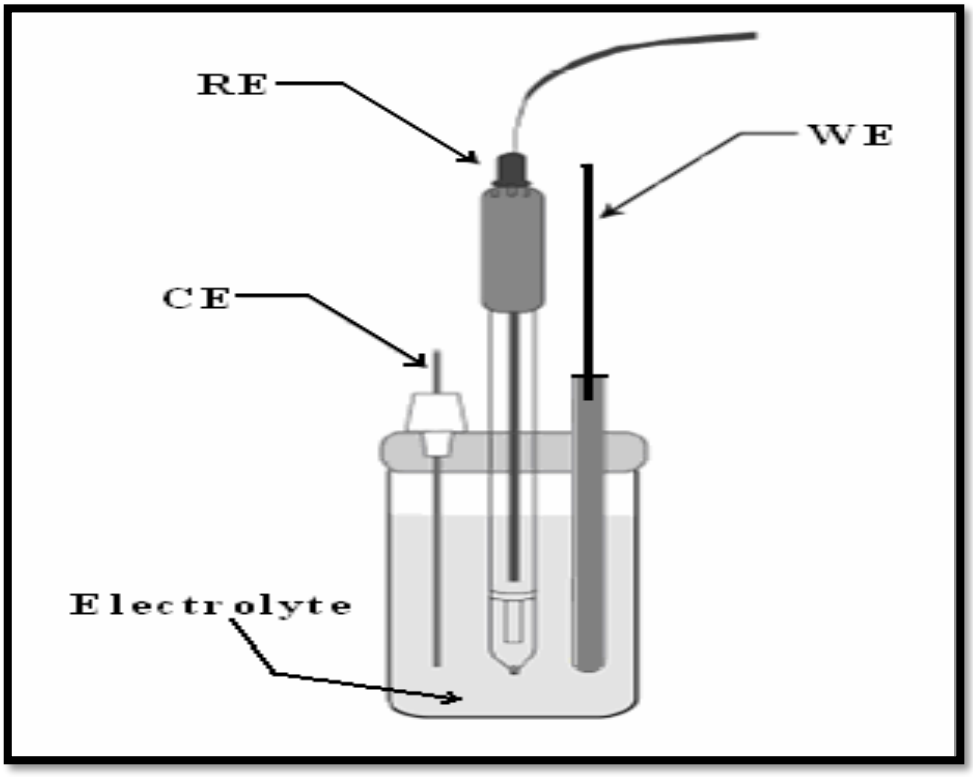


Figure (2.3): A schematic shows one compartment three electrodes electrochemical cell.

The measurements of cyclic voltammetry (CV) were prepared at room temperature in a cell containing 0.5M KOH electrolyte. The potentials witches between -650 and 650 mV, against Ag/AgCl reference electrode, at a scan rate of 50 mV/s and ten cycles were registered for every electrochromic film. The immersed film area in the electrolyte was kept to be ~ one cm^2 during all CV measurements.

2.2.2 Chronoamperometry (CA)

Chronoamperometry is an electrochemical technique where the working electrode potential is stepped and the resulting current occurring at the electrode (caused by the potential step) is monitored as a time function.

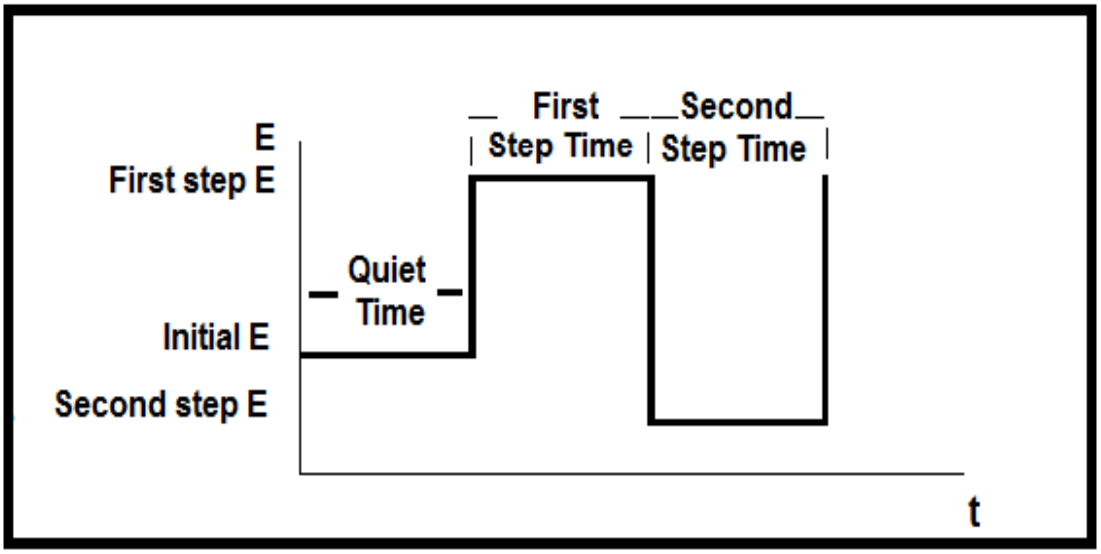


Figure (2.4): Potential wave form for chronoamperometry.

Chronoamperometry (CA) measurements for prepared films were done at room temperature. The potential varied between -0.65 V and 0.65 V, against Ag/AgCl reference electrode with 20 s for each potential. An area of one cm^2 of electrochromic prepared films was immersed in KOH electrolyte. For each film, twenty CA cycles have been performed.

2.2.3 Transmittance

The transmission of light through prepared NiO films was measured in a light wave length ranges from 200 to 1000 nm. Also, the light transmission using single wavelength (630 nm) was also measured. During CA measurements (coloring and bleaching).

2.3 Instruments

1- PGZ402 universal potentiostate

Chronoamperometry (CA), cyclic voltametry (CV) and chronocolumetry measurement were done by using PGZ402 universal potentiostate device.



Figure (2.5): The photos shows PGZ402 universal potentiostate instrument.

2- Shimadzu UV-3101PC UV-VIS-NIR scanning spectrophotometer

Spectrometer is an instrument study the optical properties (absorbance, transmittance, and reflectance) to provide us with information that is give solutions in the analysis of films, coatings, plastic, powders and liquids. In this thesis used transmittance measurement to calculate energy band gap and thickness for many films.



Figure (2.6): Shows shimadzu UV-3101PC UV-VIS-NIR scanning spectrophotometer device**.**

3- Elma ultra-sonicator

Ultrasonic cleaning is a technology that uses high frequency sound waves (ultrasonic: above the range of human hearing) to agitate an aqueous or organic medium (cleaning chemistry) that in turn acts on contaminants adhering to substrates like metals, glass, plastics, ceramics and rubber contaminants can be dust, dirt, oil, pigments, grease, flux agents, polishing compounds, fingerprints, soot wax and mold release agents, biological soil like blood, and so on.



Figure (2.7): : Elma ultrasonic cleaner.

4- Bifa laboratory furnaces

Bifa laboratory furnaces used to annealed many films at 300 ˚C for one hour under air.



Figure (2.8): Bifa laboratory furnaces.

5- Rikago miniflex 600 X-ray diffractometer.

X-ray diffraction is a strong tool for thin films studying because it gives many information like crystal structure, lattice constant, sample purity, and unit cell dimension. When X-rays incident on the surface of crystal, the crystal is rotated and X-rays are reflecting from many lattice planes and recorded by radiation detector.

The X-ray diffraction is depending on constructive interference of X-rays and crystalline sample. The inter action between incident rays and sample gives constructive interference when conditions satisfy brag's law.

The XRD data was obtain using Rikago miniflex 600 diffractometer as shown in figure (2.9), which consist of many parts:

1- X-ray tube: the source of X-rays with a wavelength 1.5405 ^{o}A.

2- Collimator.

3- The sample and sample holder.

4- Detector: count the number of x-rays scattered by the sample.

5 Signal processor.



Figure (2.9): The schematic shows Rikago miniflex 600 diffractometer.

Chapter Three

Results and Discussion

Chapter Three

Results and Discussion

Nano-particles of Ni-based semiconducting electrochromic thin films have been prepared by electrochemical deposition technique. The effects of cleaning processes, different molar concentrations and different deposition voltages on the prepared films characteristics (optical, electrochromic and structural) have been studied. The films have been characterized using different measuring techniques listed below:

1- Cyclic Voltammetry (CV).

2- Chronoamperometry (CA).

3- Optical Transmission Spectra.

4- X-ray analysis.

3.1 Effect of cleaning process: adhesion and uniformity of Ni-based films

In the deposition of Ni-based thin films on FTO substrate, the important thing before the deposition of these films were cleaning substrate from any impurities or dirt to achieve desirable properties of the film like homogeneous, adhesive and high electrochromic properties.

In thin film technology, adhesion is very important to determining the durability of deposited thin film. The durability and longevity for thin films are largely depending on their adhesion to the substrate because this

determines the removal ease. It is desirable that these films should be capable of being polished and cleaned.

Wear depends on adhesion extent of thin film to the substrates; if the adhesion is poor, the film will wear off quite rapidly. Cleaning of the substrate plays an important role to increase adhesion of the film to substrate and protect it from wearing off.

As previously described in the experimental part, different cleaning processes have been tested to study the effect of cleaning on the film adhesion and characteristic.

For different films, prepared at different cleaning processes (M_1, M_2, M_3, M_4, M_5, M_6, M_7), normal and magnified photos were taken to study homogeneity and adhesion to the substrate.

The photos for films were taken for as prepared films (before annealing (B)) and for films post annealed, at 300 ^{o}C for one hour under air (after annealing (A)). Normal photos for prepared films (As deposited and post annealed at 300 ^{o}C for one hour under air are shown in (Fig. 3.1).

As may be seen in figure (3.1 a), films deposited on to cleaned substrates using dish washing liquid alone, or followed by using single solvent (isopropanol, aceton, or ethanol) treatment and coupled with ultrasonic machine, are not homogeneous. Some of them showed partially wearing off of the films. These films are represented by cleaning methods (M_1, M_2, M_3, M_4, and M_5) respectively. On the other hand, films deposited on substrates cleaned by successive ultrasound cleaning in isopropanol, aceton, and ethanol have higher homogeneity and adhesion to the substrates. After

annealing of the films (Figure. (3.1 b)), the films deposited on substrates cleaned by first four methods (M_1, M_2, M_3, and M_4) were weared off and only small isolated zones remain on the substrates.

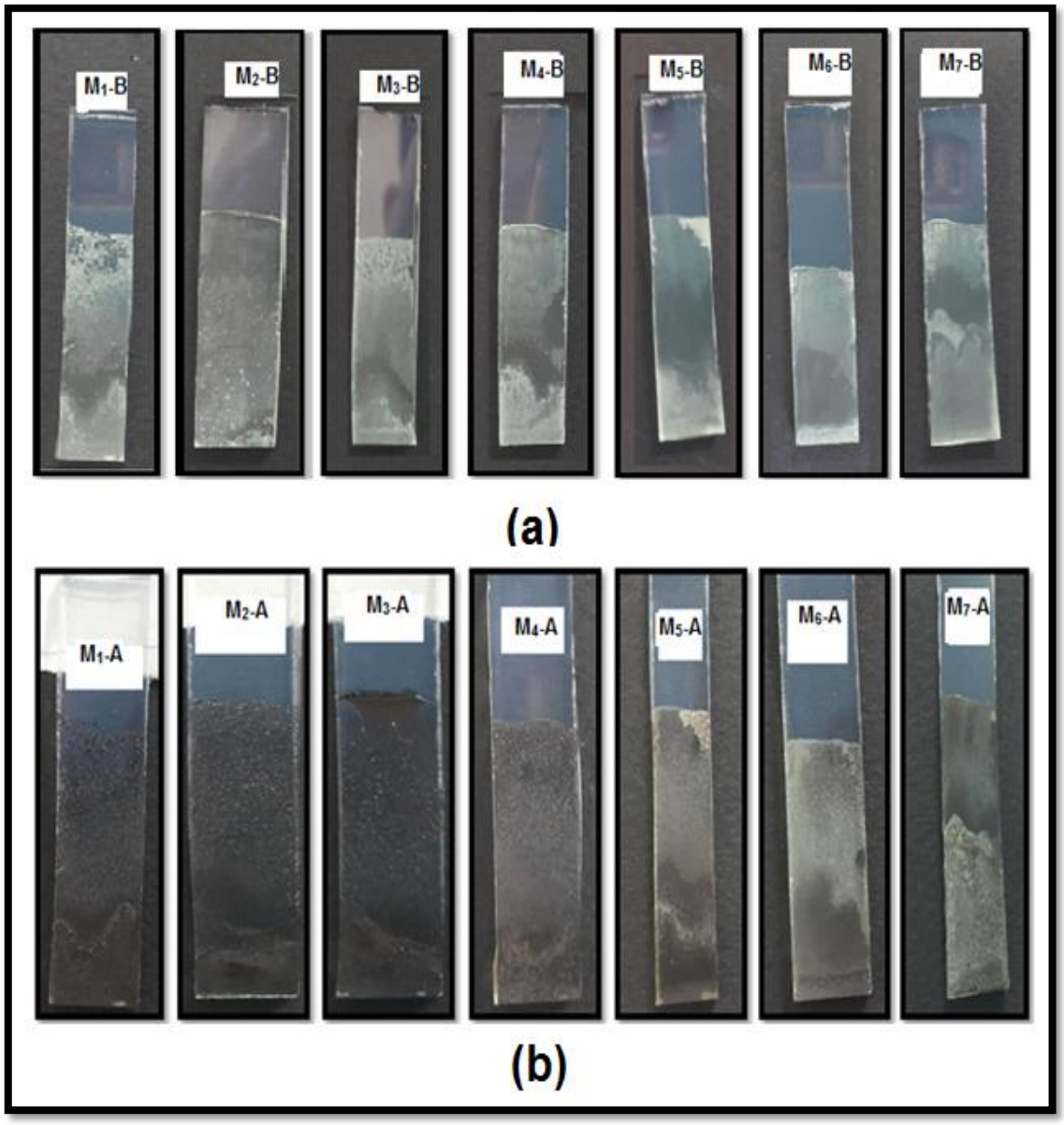


Figure (3.1): Normal photos for different prepared films at different cleaning process: a) as deposited films (B: before annealing) and b) films after post annealing at 300 ^{o}C for one hour under air (A: after annealing).

Higher magnified photos for as deposited films before annealing (films B) obtained using optical microscope are shown in figures (3.2 and 3.3) for

x100 and x400 magnification, respectively. Figures (3.2 and 3.3) shows that all films have growth of the type 3D island growth (volmer, weber) in this growth process, atoms are agglomerate together on the substrate in a form of separated film islands.

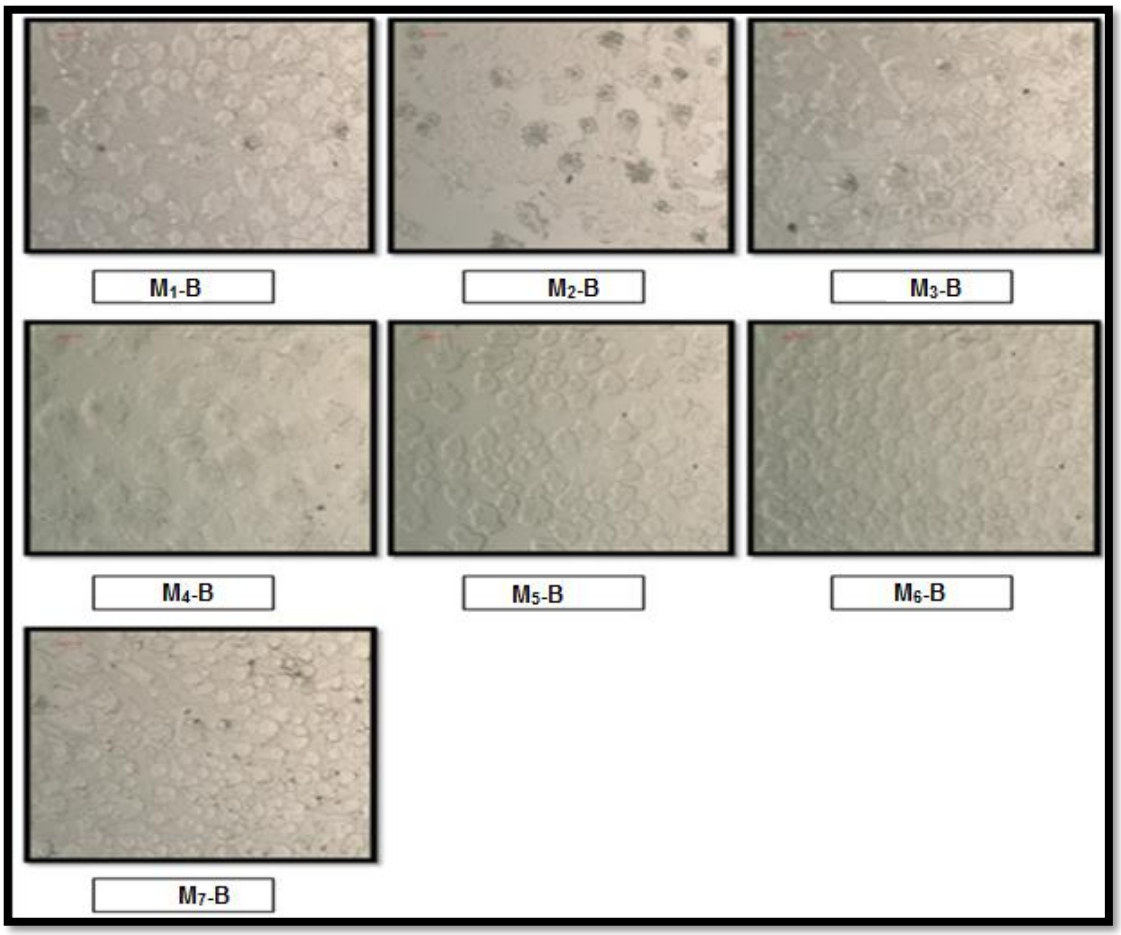


Figure (3.2): Microscope photos (×100 magnification) for as prepared films with different cleaning processes before annealing (B).

As the growth continues, islands become larger and extends to cover the substrate with the film material [66]. In this growth method, atoms are more strongly bound to each other than to the substrate. Films deposited on substrates, cleaned by M_1, M_2, M_3, M_4, and M_5 shows that formed films island are not connected together and hence, the films are not fully cover

the substrates. On the other hand, films deposited on substrates cleaned by M_6 and M_7 show that the films islands are connected together forming larger regions covers that the substrate better. It is worth notice that the films deposited substrates cleaned by M_6 method have the widest covered, continuous, and homogeneous regions have the coverage, continuity and homogeneity. In addition, figure 3.3 (x400 magnified) photos shows that many cracks exist in the films deposited on substrates cleaned by M_1, M_2, M_3, M_4, and M_5.

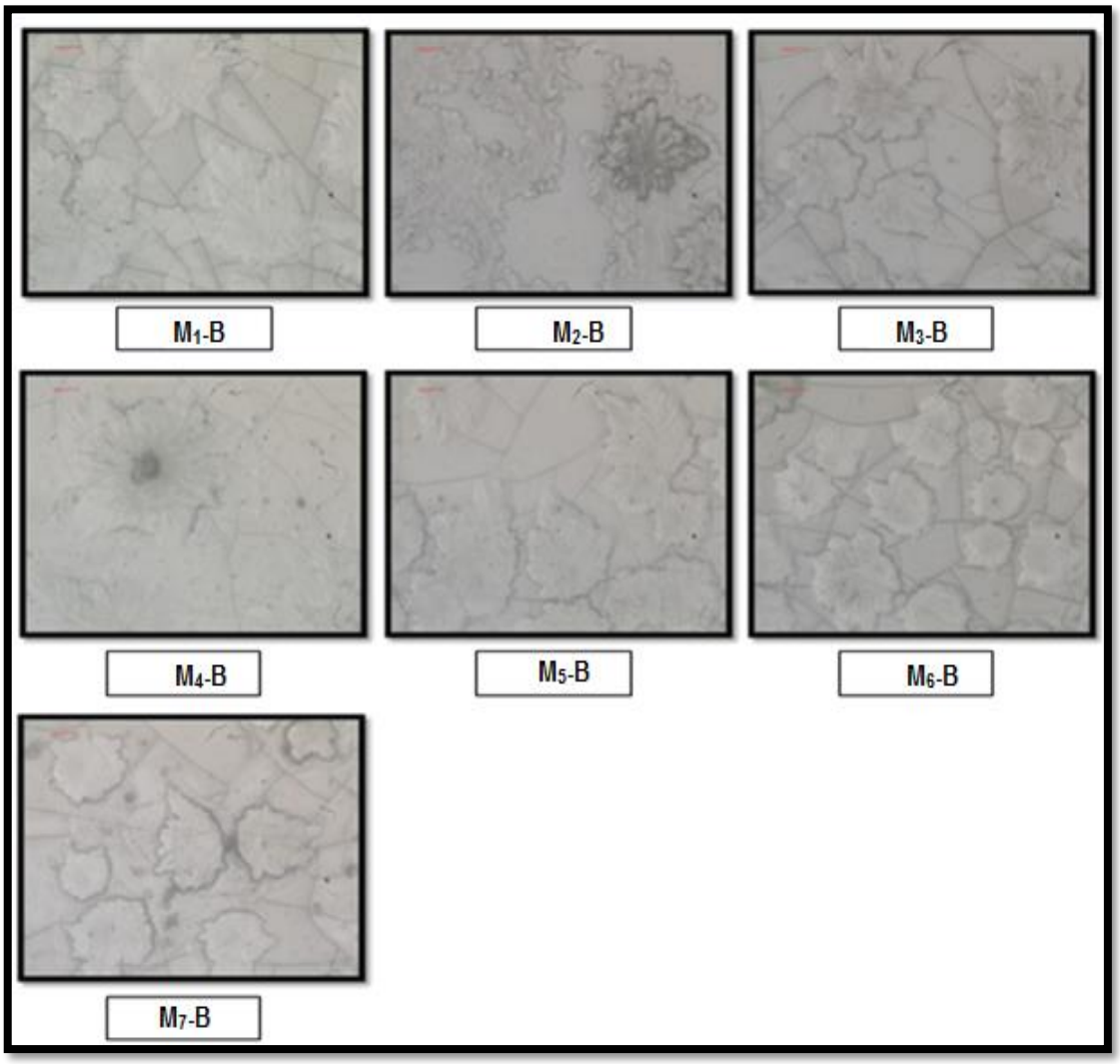


Figure (3.3): Microscope photos (× 400 magnification) for as prepared films with different cleaning processes before annealing (B).

High magnification of annealed films (films A) are shown in figures (3.4 and 3.5) for magnification of x100 and x400 respectively. For these images the films deposited on to substrate cleaned by M_1, M_2, M_3, and M_4 showed many cracks and exhibited wearing off phenomena. It is known that annealing will lead to densification and hence shrinkage of the material [56]. As previously mentioned, in 3D island growth, film atoms are more strongly bound to each other than the substrate, shrinkage due to densification is observed to lead to agglomeration of islands together and wearing off from substrate. On the other hand, films deposited on other substrates cleaned by (M_5, and M_6) showed some voids in the films with densification process and no insulating cracks were observed.

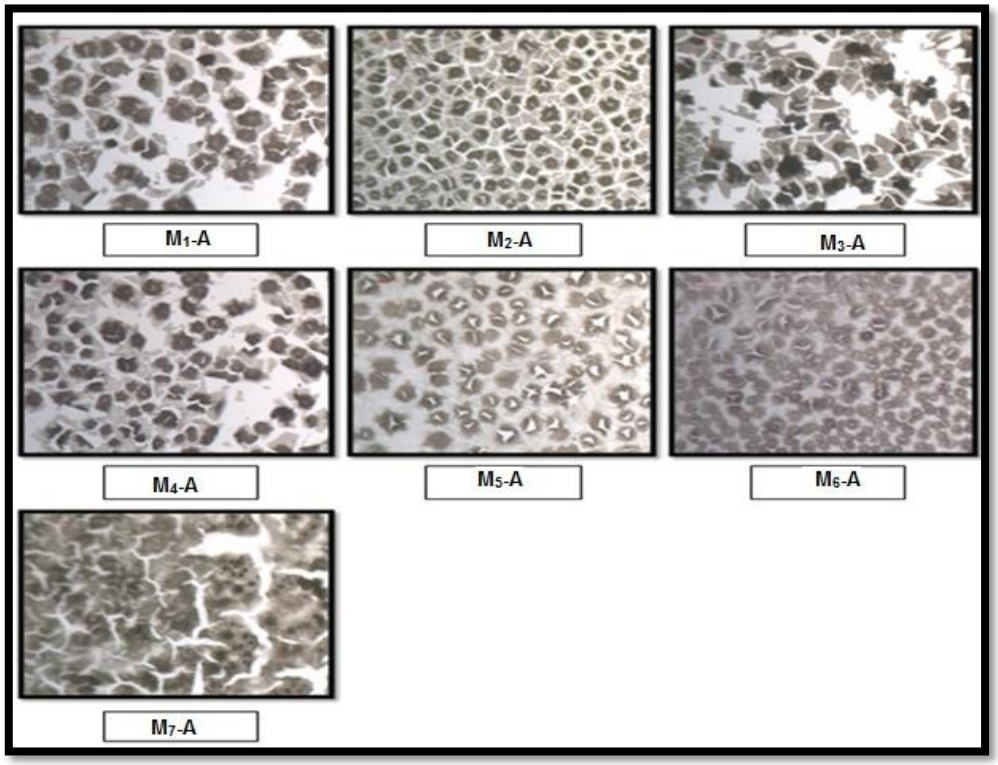


Figure (3.4): Microscope photos (×100 magnification) for films after post annealing at 300 °C for one hour under air with different cleaning processes after annealing (A).

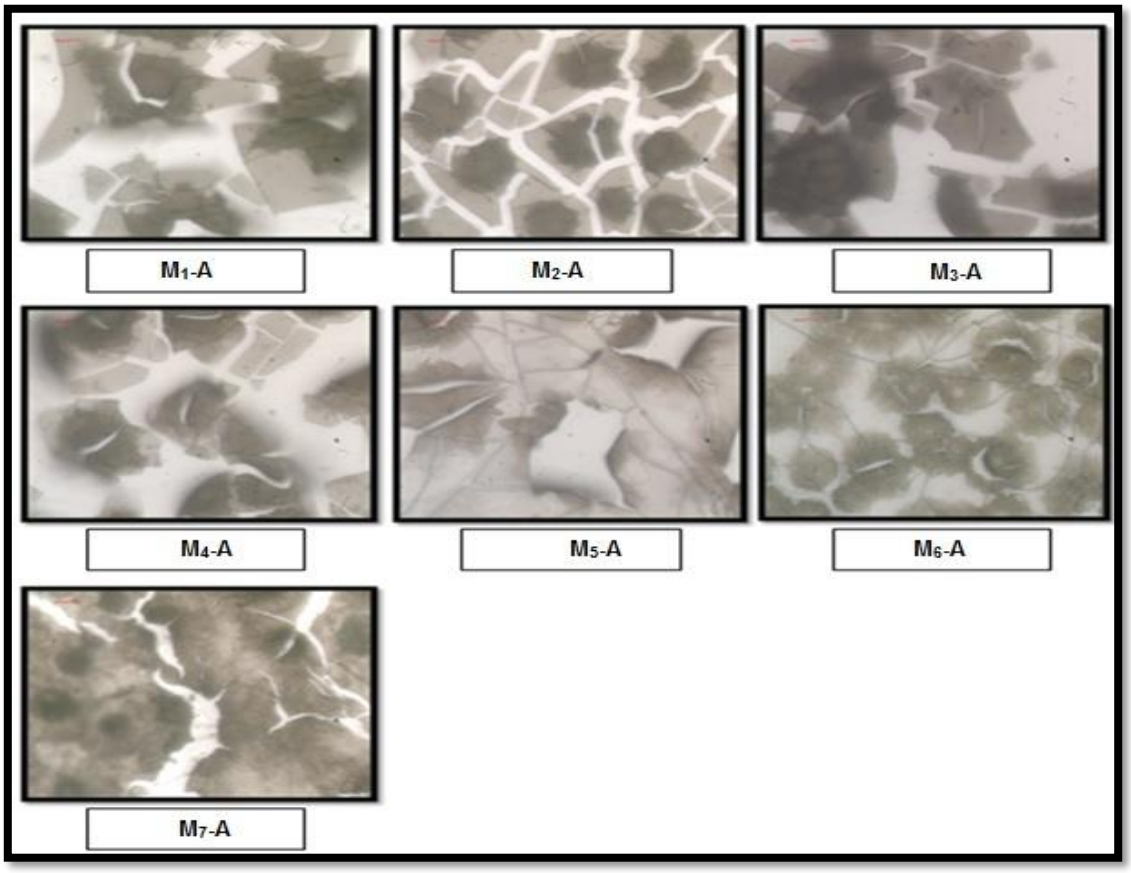


Fig. (3.5): Microscope photos (×400 magnification) for films after post annealing at 300 ^{o}C for one hour under air with different cleaning processes**.**

Film deposited onto substrates cleaned by M_6 methode have the least voids and the highest homogeniouty. The not wearing off the films may be because of the growth is not pure 3D island. But it is more probably to have stranski-krastanov type, which is a mix growth between layer by layer growth followed by 3-D island. In this growth method, atoms are strongly bound to each other and to the substrate [66]. Hence M_5, and M_6 cleaned substrate have not wearing off of the films and they are well attached to the substrates. It is also observed that the films prepared by M_6 method exhibit high homogeneity, less cracks, and large coverage area.

For films deposited onto substrates prepare by M_7 method. After annealing, they show high surface area agglomeration of film material. But unfortunately, major large crakes are observed. It is believed this film have same growth type as those cleaned. But, due to the presence of HF acid in the cleaning process, the substrate was highly etched and probably damaged. Moreover, as observed by eye, the substrate begins to dissolve since it is made from glass with thin layer of FTO. HF will affect FTO conductivity and the glass begins to dissolve even if we have diluted HF acid [67].

As a conclusion, electrochromic thin films deposited on substrates cleaned by method M_6 showed highest homogeneity, continuity, and adhesion to the substrate for both before and after annealing of the films. Cleaning method 6 (M_6) steps are re-described here after:

1- Cleaning (FTO/glass) sample with dish washing liquid (Fairy dish washing liquid 2.5 ml in 50 ml tap water) to remove any attachments or dust. Washing (FTO/glass) sample with tap water after that washing in deionized water to remove fairy liquid.

2- Drying (FTO/glass) sample with pressed air and putting (FTO/glass) sample in isopropanol on sonicator for ten minutes and washing with deionized water, then drying (FTO/glass) sample with pressed air and putting in aceton on sonicator for ten minutes.

3- Washing in deionized water, then drying (FTO/glass) sample with pressed air and putting in ethanol on sonicator for ten minutes. Washing

with deionized water, then drying (FTO/glass) sample with pressed air and putting HCL for two minutes on (FTO/glass) sample.

4- Washing (FTO/glass) sample with deionized water and drying (FTO/glass) sample with pressed air. Drying (FTO/glass) sample at 100 °C for five minutes.

This substrate cleaning method is used for all coming prepared films to study different parameter effect on electrodeposited Ni-based film. The reason for M_6 being the best method is that we have used many solutions in the cleaning process to ensure removal of all contaminants that may exist on the substrate. Cleaning with dish washing liquid followed by tap water and deionized water washing (step 1 of M_6) will ensure removal of any dust attachment and washing liquid. The following of the steps in M_6 procedure (step 2 and 3) will remove and/or dissolve any attached glue, grease, proteins, oils, and lipids; acetone solvent is a great cleaner to dissolve almost any glue attachment to substrates. It is also known to be a heavy duty degreaser. Isopropanol and ethanol are usually used in cleaning to denaturing proteins and dissolving lipids [67]. HCL then was used in cleaning process. This will result in a hydrogen –terminated hydrophobic surface. In addition, acid will make etching for the substrate, which makes surface rougher, and hence larger number of nuclei in deposition. This in turn may lead to smaller grain size [68]. The other cleaning methods show less surface continuity, less homogeneity, and less adhesion due to the fact that there is still contaminants on surface that disturb uniform growth of the film and hence less film quality were obtained.

3.2 Electrodeposition potential optimization for Ni-based electrochromic thin films.

Ni-based thin films were deposited onto M_6 cleaned FTO/Glass substrates using different electrodeposition potentials. The electrochemical deposition of the films was performed by using chronocolometry at -500, -600, -700, -800, and -1000 mV. The deposition continues until a total charge of -5 C was deposited. The deposition area for the film (immersed area in deposition solution) was two cm^2 (2×1 cm^2). The concentration of $Ni(NO_3)_2.6H_2O$ in the aqueous solution was 1M. For each potential three samples were prepared to perform the different experiments needed.

3.2.1 $Ni(OH)_2$ electrochromic films

Deposition of the films, using electrodeposition, in the electrochemical cell will result in having films of nickel hydroxide ($Ni(OH)_2$). The reactions have place during deposition is given by [69]:

$$NO^-_3 + 7H_2O + 8e^- \longrightarrow NH^+_4 + 10OH^- \quad (3.1)$$

$$Ni^{2+} + 2OH- \longrightarrow Ni(OH)_2 \quad (3.2)$$

3.2.1.1 $Ni(OH)_2$ chronoamperometry (CA)

Chronoamperometry measurements were done for as deposited films before annealing (B-films) and for films after annealed at 300 °C for one hour under air (A-films). twenty cycles of CA were performed in 0.5M KOH. The potential was cycled at -650 mV and 650 mV versus Ag/AgCl reference electrode. Each cycle potential was kept for a duration of 20

seconds. CA cycles for films before annealing ($Ni(OH)_2$ B-films) are shown in (Fig. 3.6).

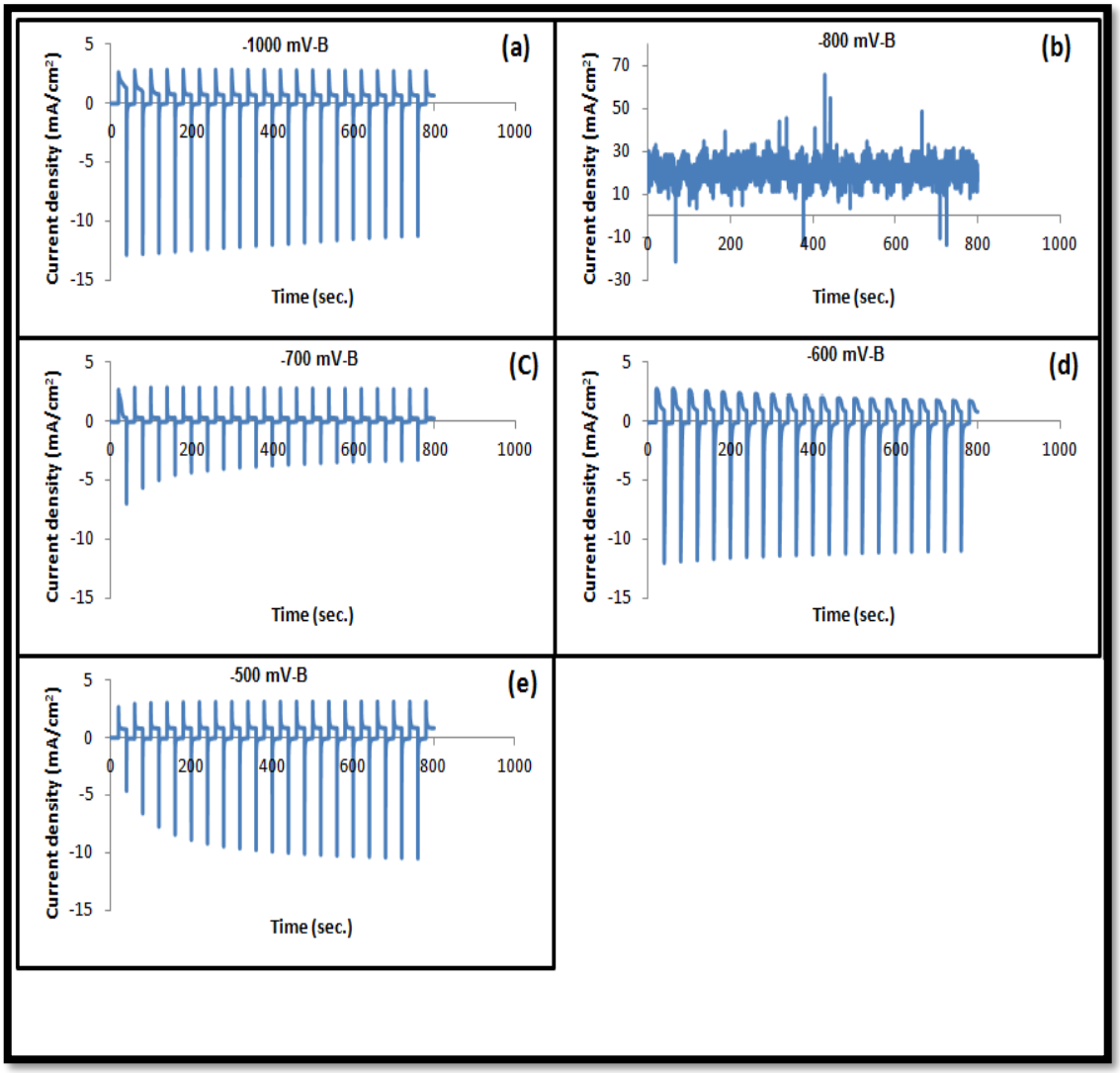


Figure (3.6): CA curves during twenty cycles for $Ni(OH)_2$ films deposited at deferent deposition potentials. Potential cycled between -650 mV and 650 mV versus Ag/AgCl reference electrode in 0.5 M KOH electrolyte.

Films deposited at potentials -500, -600, -700, and -1000 mV show a stability in anodic current density peaks (J_a), cathodic current density peaks (J_c), and graph shape during CA cycles. On other hand, there is no stability in J_a, J_c, and shape for films deposited at -800 mV. CA measurements are

used to deduce many parameters like anodic charge density (Q_a), cathodic charge density (Q_c), coloration time (t_c) and bleaching time (t_b). Q_a and Q_c can be deduced by integration of J_a and J_c respectively in the current density Vs. time graph. A schematic figure (3.7.a) shows how to find Q_a and Q_c from the integral of J-t graphs according to the following equation:

$$Q = A \int J dt \qquad (3.3)$$

Coloration time (t_c) and bleaching time (t_b) can be found from the time needed to stabilize the J_a and J_c, respectively, to an essentially constant value near zero. Figure (3.7.b) shows a schematic explanation for how to find coloration and bleaching time. For our CA experiments Q_a, Q_c, t_c, and t_b which are deduced from cycle twenty are shown in table (3.1). Cycle twenty is chosen to ensure stabilization of electrochemical oxidation reduction during CA measurements that are also shown in Fig. (3.7.a).

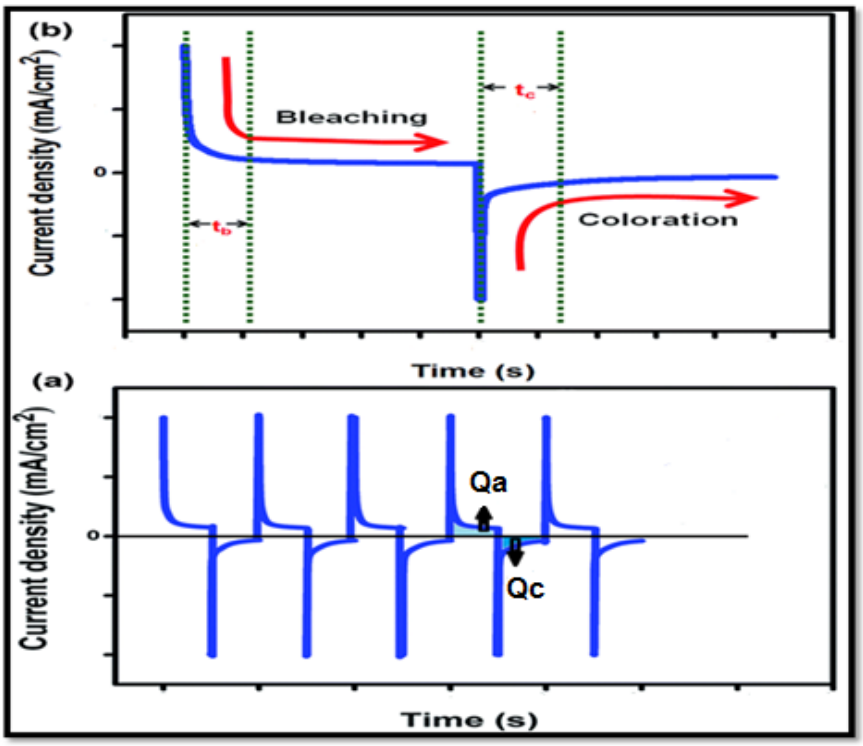


Figure (3.7): The shematic explains how to find Q_a, Q_c, t_b and t_c values.

3.2.1.2 $Ni(OH)_2$ transparency during CA measurements

During CA measurement, transparency measurements have been performed at light wavelength of 630 nm. Transparency measurements have been performed to measure the film transparency of light in color (T_c) and bleach (T_b) states during electrochromic process that takes place while CA measurement are running.

In addition, transparency during CA represents other way to find t_c and t_b. A schematic which explains how to find T_c, T_b, t_c, and t_b is shown in (Fig. 3.8).

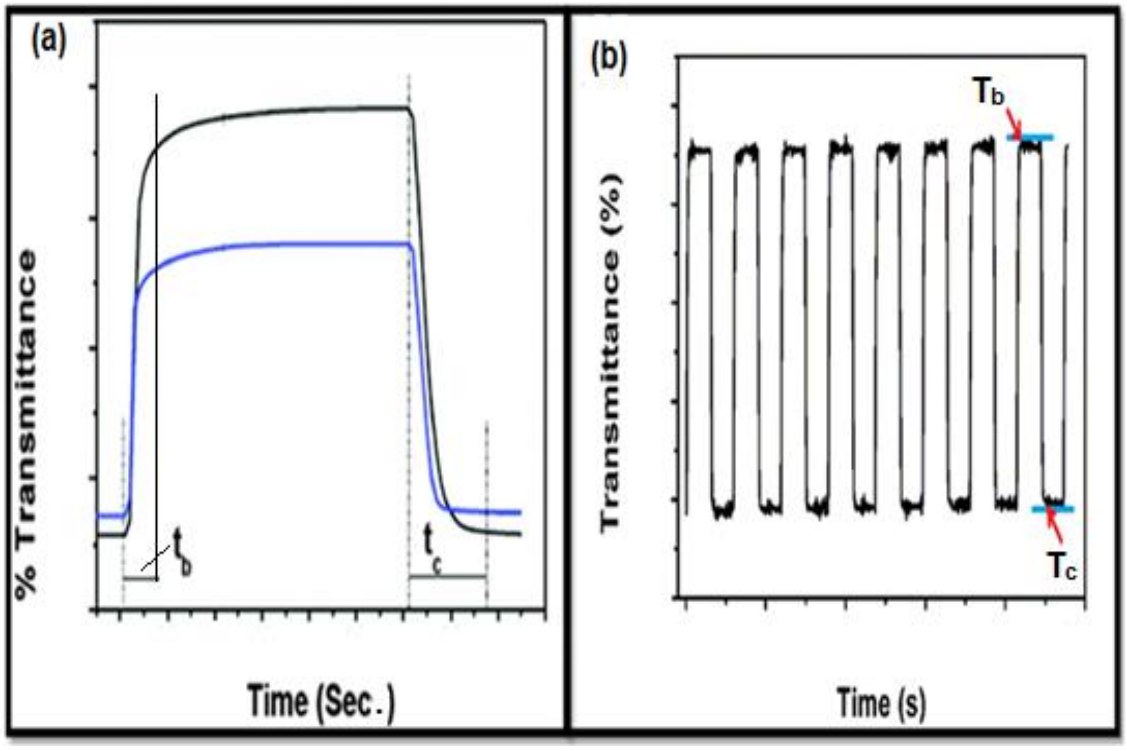


Figure (3.8): The schematic shows how to find T_b and T_c also t_b and t_c.

The transparency measurements during CA experiments of $Ni(OH)_2$ films deposited at different deposition voltages are shown in (Fig. 3.9).

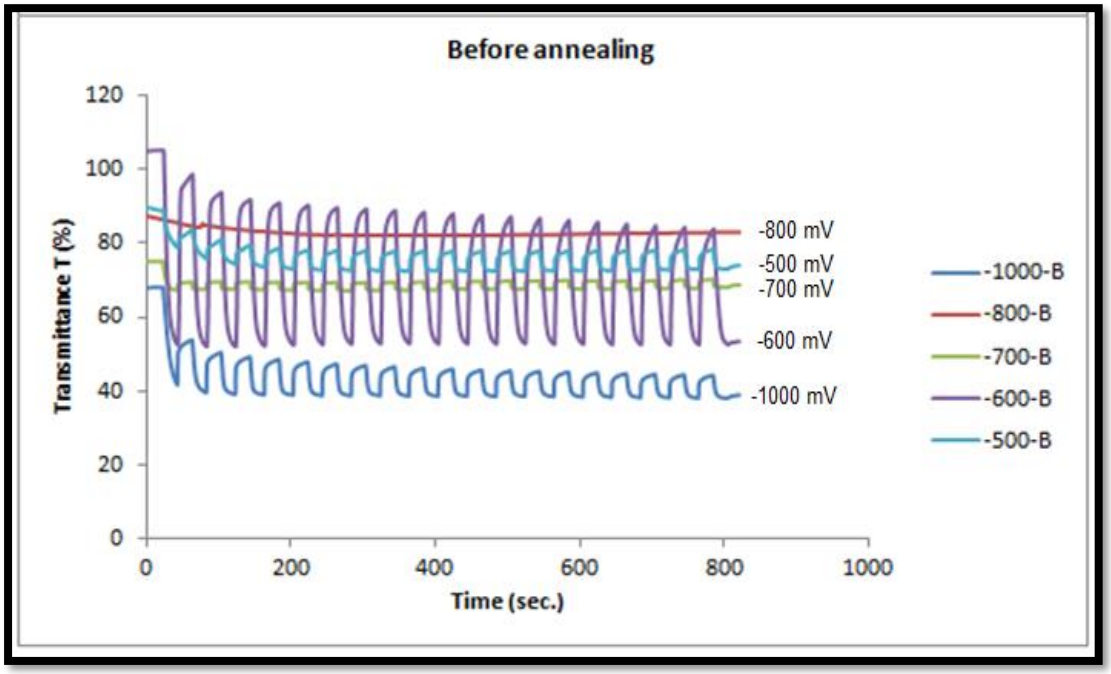


Figure (3.9): Optical transmittance change at 630 nm wave length during CA for $Ni(OH)_2$ thin films deposited at different potentials.

Weak coloration bleaching has been observed, in the figure (Fig. 3.9), for all the films except those deposited at -600 mV. It is obviously shown that the coloration bleaching difference for this film (deposited at -600 mV) have the highest transparency difference. Hence, one could expect that this film has best electrochromic parameters.

Indeed, the coloration bleaching process during CA measurements takes place according to the following reaction:

$$Ni(OH)_2 + OH^- \leftrightarrow NiOOH + H_2O + e^- \quad (3.4)$$

Where $Ni(OH)_2$ is transparent but NiOOH is colored.

From transparency measurements of prepared films, T_c and T_b are found for cycle twenty and tabulated in table (3.1).

3.2.1.3 $Ni(OH)_2$ electrochromic parameters

Data collected in table (3.1) were used to calculate different electrochromic parameters. Reversibility of intercalating charges, is defined as the ratio between cathodic and anodic charge densities (Q_c/Q_a). It is known that the best reversibility is achieved when having Q_c/Q_a approaching unity with ideal value of $Q_c/Q_a = 1$.

Other parameter, which is the contrast ratio (T_b/T_c), can be deduced. The highest the contrast ratio, the better electrochromic performance of the film. Moreover, coloration efficiency (CE) is usually calculated from data recorded in table (3.1). Coloration efficiency is calculated using the following formula (described before in chapter one):

$$CE = \frac{\Delta OD}{Qc} = \frac{1}{Qc} \log \frac{Tb}{Tc} \qquad (3.5)$$

Q is the injected charge density to switch the electrochromic film material from bleach state to color state. In our case Ni-based films ($Ni(OH)_2$ or NiO) have anodic (when connected to anode) coloration characteristics; the injected charge will be $OH^-(Q_c)$ to change $Ni(OH)_2$ transparent film to NiOOH color film. Hence, Q_c will be used in above equation (3.5) to calculate CE.

The calculated parameters reversibility, contrast ratio, and coloration efficiency are also tabulated in table (3.1).

Table (3.1): Deduced and calculated electrochromic parameters for films before annealing ($Ni(OH)_2$) deposited using different deposition potentials (mV).

V (mV)	Q_c (C/cm^2)	Q_a (C/cm^2)	T_b (%)	T_c (%)	t_b (sec.)	t_c (sec.)	Reversibility (Q_c/Q_a)	T_b/T_c	CE (cm^2/C)
-1000-B	6.10	16.79	44.5	38.4	3.9	4.9	0.36	1.16	10.6
-800-B	-	-	-	-	-	-	-	-	-
-700-B	1.29	6.92	71.6	68.2	2.9	5.9	0.19	1.05	16.4
-600-B	20.75	27.15	83.9	52.7	12.8	9.8	0.76	1.59	9.7
-500-B	6.09	19.68	78.7	73.3	4.9	4.9	0.31	1.07	4.8

From table (3.1), one can see that the film that gives best electrochromic parameters (highest contrast ratio (1.59), highest reversibility (0.76), high coloration efficiency (9.7), and highest coloration difference (T_b-T_c)) was for the film electrodeposited at -600 mV, as expected before. For higher deposition voltages, all electrochromic parameters showed less values than that for -600 mV. In electrodeposition, it is known that the potential highly affects the film crystallinity, morphology, grain size, adhesion, etc. [70, 71]. Electrodeposited films usually have a potential range for good quality films. However, at higher potentials, the electric field strength increases within the cell and this accelerates the ion transport for deposition on FTO/Glass substrate. The accelerated ion transport results in higher duration shrinkage, cracking and less adhesion to substrate during

deposition. It indeed negatively affects the electrochromic parameters at high potentials. Such behavior may be a reason for instability in CA measurements for film deposited at -800 mV or higher.

To confirm our results and discussion, linear sweep voltammetry (Fig. 3.10) have been done to deposit $Ni(OH)_2$ film from $Ni(NO_3)_2.6H_2O$ the electrodeposition begins to take place at potential value of -300 mV as shown. However, the current density becomes almost linear between -500 and -700 mV. This indicate the optimal potential range for $Ni(OH)_2$ electrodeposition. At potentials values higher than -700 mV, the current density increases rapidly due higher speed particles at higher electric field and also oxidation of Ni^{+2} to Ni^{+3}. Increasing the potential at -800 mV, the Ni^{+3} production enhances in a form of NiOOH. However, when the potential increased up to -1000 mV, the Ni^{+3} (NiOOH) production is dominated [72, 73].

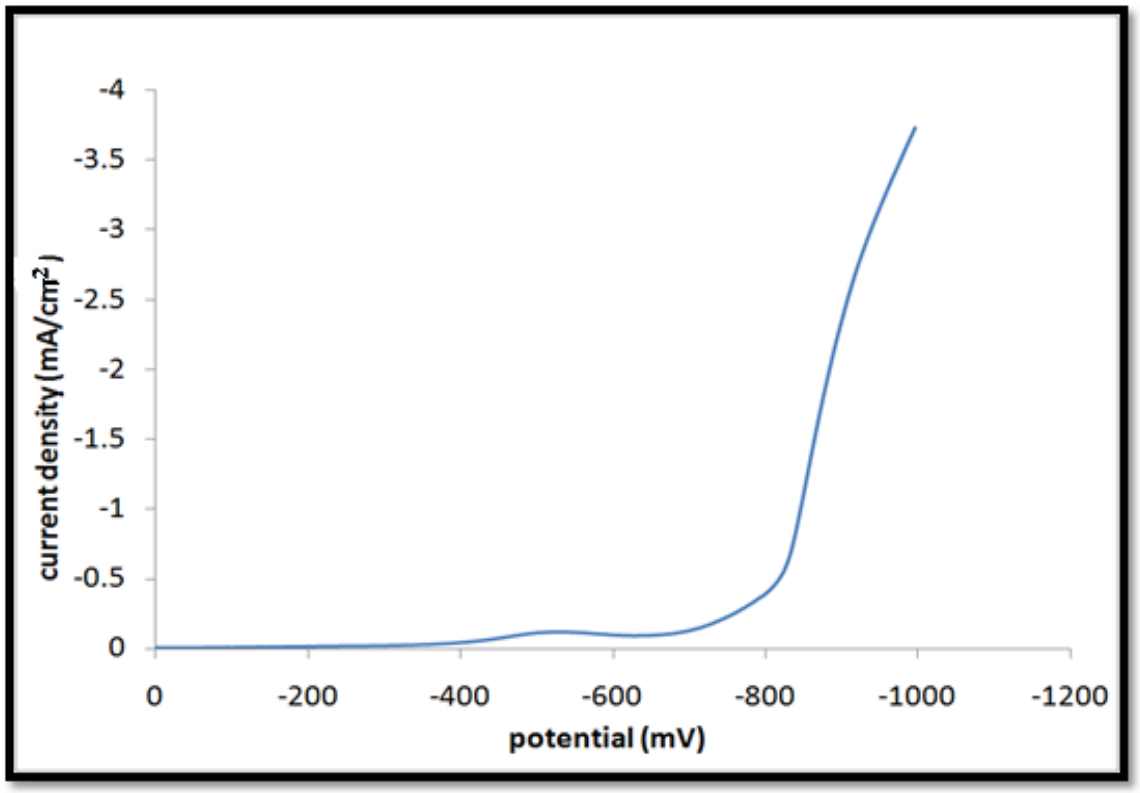


Figure (3.10): Linear sweep voltammogram for $Ni(NO_3)_2.6H_2O$ solution done at 50 mV/s versus Ag/AgCl reference electrode.

3.2.1.4 Optical parameters

For $Ni(OH)_2$ thin films deposited at different deposition potentials, transparency measurements have been performed using light wavelength ranges from 200-1000 nm (Fig. 11).

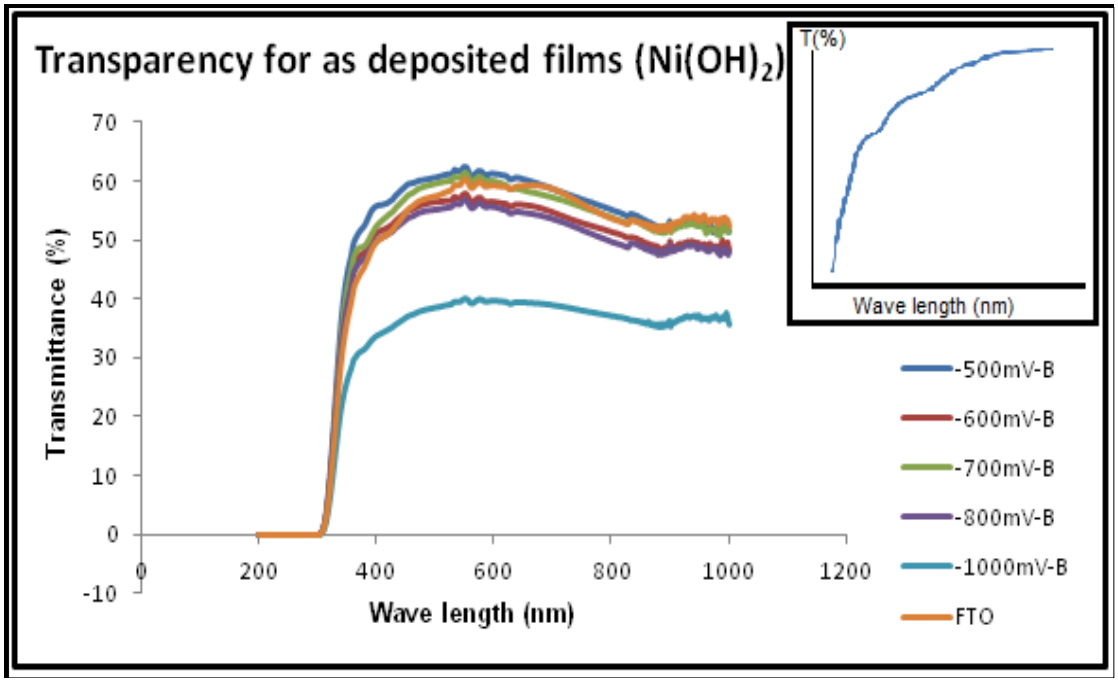


Figure (3.11): Transparency spectra for $Ni(OH)_2$ deposited at different deposition potentials. The inset shows the fringes for film deposited at -600 mV.

Relative to FTO/Glass substrate, almost all films show a high transparency in the visible and near-infra-red regions, except for that deposited at -1000 mV. This is expected due to the fact that deposited films ($Ni(OH)_2$) are in their bleach transparent coloration state [36, 39-42]. The observed decrease in transparency (highest decrease for -1000 mV deposited film) as increasing potential may be due to increase in defect density while depositing the film, and/or introducing other phase related to Ni^{3+} oxidized state (like NiOOH). The transparency spectra were used to investigate both thin films thickness and their optical band gap (E_g).

a) Thin film thickness calculations.

The interference fringes observed in the transmittance spectrums were used to find the Ni-based thin films thickness. When the light hits a thin film both the bottom and top surfaces of the film reflect light. Therefore, the

reflected light total amount are based on the sum of two reflections. Furthermore, because of the wave-such as nature of light, according to these two reflections phase may constructively or destructively add to each other. The appeared fringes in the resulting interference form can be used to determine the film thickness using the following expression [74]:

$$d = \frac{m}{2D_n\sqrt{(n^2 - sin^2\theta)}} \quad (3.6)$$

where

d = film thickness

m = number of fringes in wave number region used

n = refractive index at different wavelength for different films were deduced from other works [75-77].

θ = angle of incidence.

D_n = wave number region used ($\frac{1}{\lambda_1} - \frac{1}{\lambda_2}$; cm^{-1})

Using interference fringes of transparency spectra (Fig. 3.11), the films thickness for different prepared films are calculated and tabulated in table (3.2).

Table (3.2): Calculated thickness for $Ni(OH)_2$ films deposited using different deposition potentials.

V (mV)	Film thickness (nm)
-1000 mV	675
-800 mV	669
-700 mV	698
-600 mV	698
-500 mV	705

It is clear that the thickness values of the films are close to each other. Indeed, since the deposition charge was the same for all films (5 C), then it is expected that all films must have almost the same thickness.

b) Optical band gap determination

In the strong absorption region, energy band-gap determination must obviously be considered. Ni-based electrochromic films are transparent in their bleach state (as prepared). Hence, they are expected to have large energy band-gaps, in the range of 3 to 4 eV, that correspond to photon wavelength range of about 300–400 nm (near-ultraviolet region). While photons are absorbed, they induce electronic transitions from the valence band to the empty energy states in the conduction band. In this region, one can evaluate the optical band-gap value by the following relation [78, 79]:

$$\alpha h\nu \propto (h\nu - E_g)^{\eta} \quad (3.7)$$

where $h\nu = (1240/\lambda\ (nm))$ is the photon energy, α is the absorption coefficient, η is a constant having the values 2, 1/2, 3, and 3/2 based on whether the optical transitions are indirect allowed, direct allowed, indirect forbidden and direct forbidden transition respectively. For the direct allowed transition, the linear part of the curve has to be extrapolated to zero, in order to find the E_g value for the graph $(\alpha h\nu)^2$ versus $h\nu$. For the indirect allowed transitions, the drawn curve has to be extrapolated to zero, to determine the E_g, from the graph $(\alpha h\nu)^{1/2}$ versus $h\nu$ [78, 79]. In the strong absorption region, the transmission T can be defined by the following equation [80]:

$$T \propto \exp(-\alpha d) \quad (3.8)$$

The absorption coefficient (α) could be directly calculated from the film thickness (d) and its transmission (T). For different films, of given thickness, deposited on FTO/glass substrate, absorption coefficient (α) was calculated using transparency spectra (Fig. 3.11) at different wavelengths. In order to determine the optical band gap (E_g) of Ni-based films from the graph $(\alpha hv)^2$ versus hv that was drown as shown in the (Fig. 3.12). In this figures direct optical allowed transition was assumed [81].

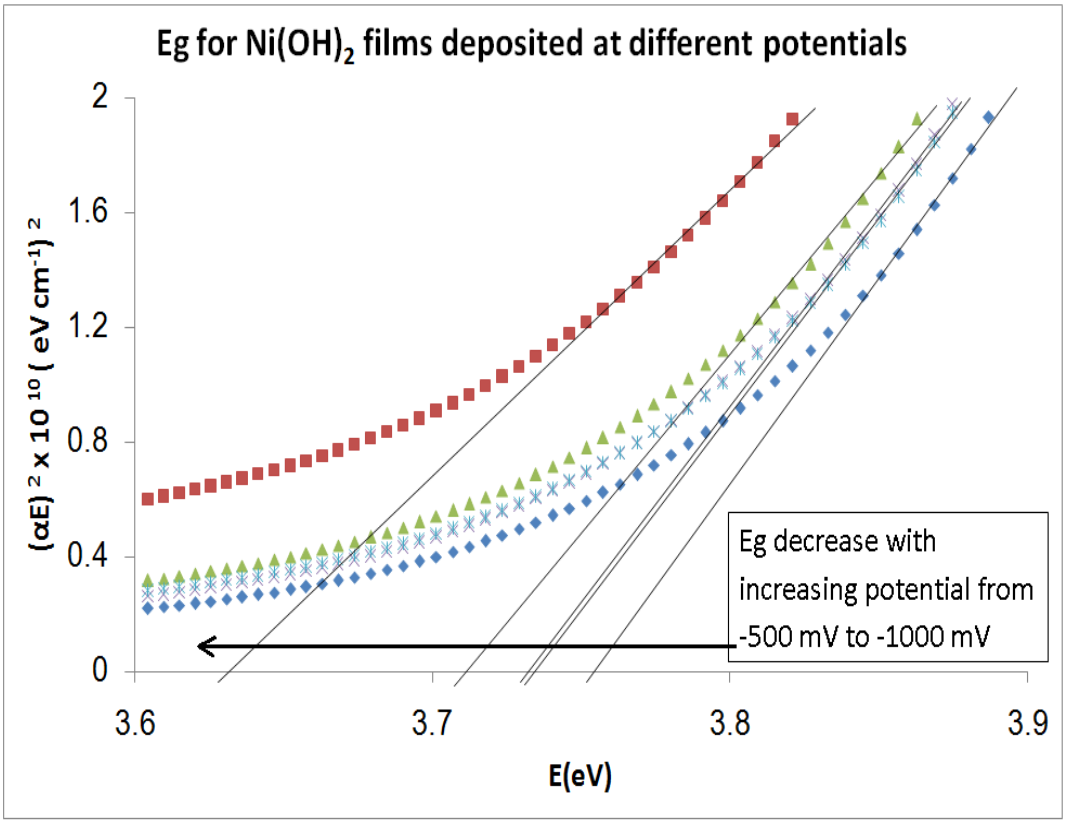


Figure (3.12): The plot of $(\alpha E)^2$ as a function of E $Ni(OH)_2$ deposited using different deposition potentials.

As shown in figure, the extrapolation of the linear part gives the optical band gap of each deposited film. The optical band gap for films deposited at different deposition potentials are recorded in table (3.3).

Table (3.3): The optical band gap for $Ni(OH)_2$ films deposited at different potentials.

$Ni(OH)_2$ Deposition potential	E_g (eV)
-500-B	3.75
-600-B	3.73
-700-B	3.73
-800-B	3.71
-1000-B	3.63

From table (3.3), E_g was found to decrease as the deposition potential increase. Indeed, (as observed in linear sweep voltammogram experiment (Fig 3.10)) increasing deposition potential from -500 mV to -1000 mV will increase the current during deposition. Increasing current will cause to have ionized particles of higher speed. Due to this, higher defect concentration will present in the film because of higher force produced during momentum change when particles collides at the substrate surface. Introducing higher defect concentration in the film will introduce higher concentration of defect energy states in the energy gap and hence reducing the optical band gap (due to inter band transition between these states) as observed in the table (table (3.3)). In addition, higher deposition potential could lead to deposition of higher grain size particles. As a result, the optical band gap will decrease due to possible increase in the thin film grain size [23]. Moreover, from figure (3.12) and table (3.3), one can observe that films deposited at -600 and -700 almost have the same E_g. This is because both potentials have same current density as also shown in the linear sweep voltammogram experiment. Moreover, all films have an optical band gap above 3.2 eV, this indicate that $Ni(OH)_2$ films are transparent in the visible rang with least transparency for films deposited at -1000 mV (see Fig.

3.11). The decrease in transparency for films deposited at -1000 mV is due to higher concentration of defects in the deposited film.

3.2.2 NiO electrochromic films

After electrodeposition of $Ni(OH)_2$ films, the films were annealed at 300 ºC for one hour under air. Annealing of electrodeposited film will transform film from $Ni(OH)_2$ to NiO. It is well known that NiO begins to calcinat at temperature of 250 ˚C and higher [82].

3.2.2.1 NiO electrochromic parameters

For NiO films, CA and transparency experiments have been done to investigate different electrochromic and optical properties. CA and Transparency during CA measurements for NiO films are shown in figures (3.13 and 3.14), respectively.

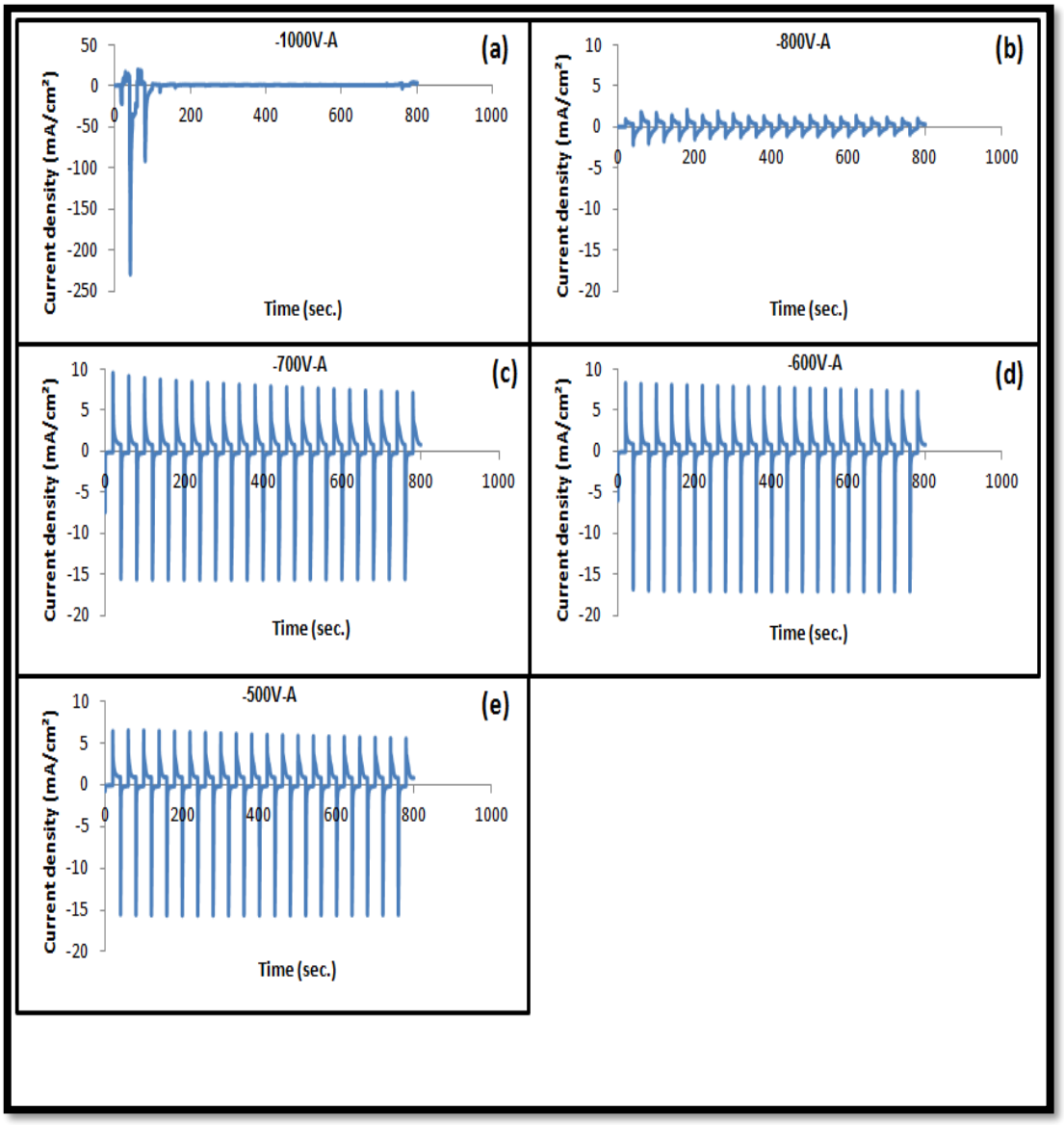


Figure (3.13): CA curves during twenty cycles for NiO films deposited at deferent deposition potentials. Potential cycled between -650 mV and 650 mV versus Ag/AgCl reference electrode in 0.5 M KOH electrolyte.

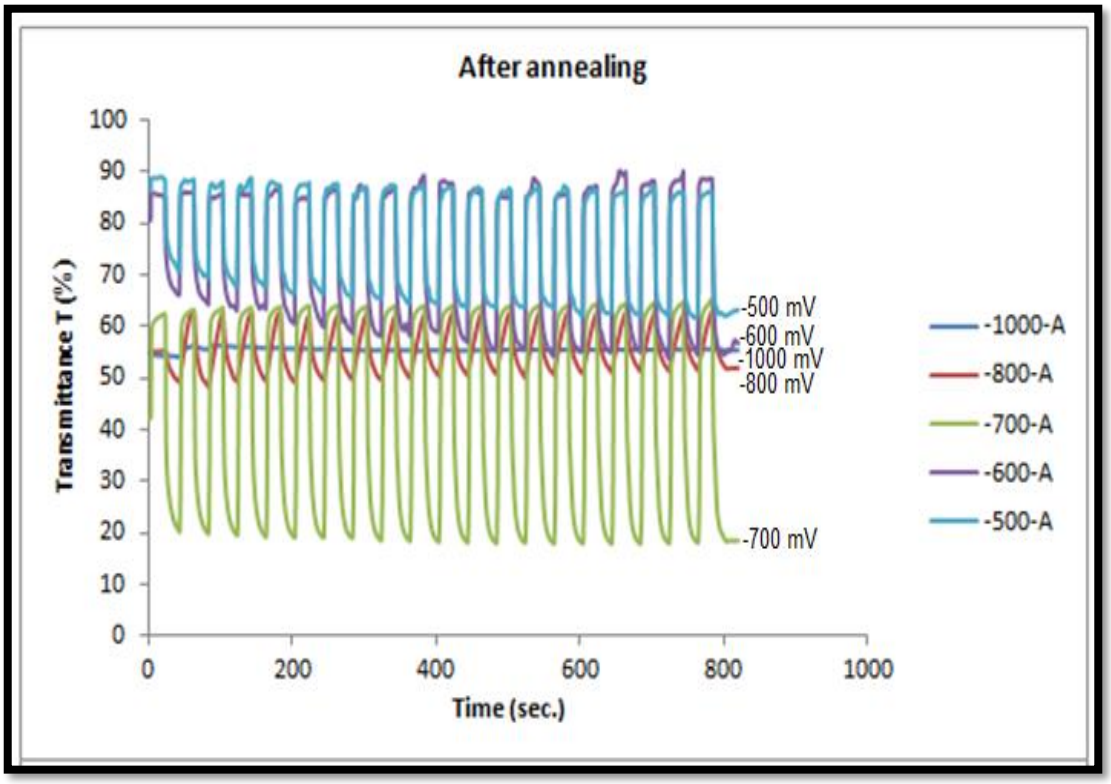


Figure (3.14): Optical transmittance change at 630 nm wave length during CA for NiO thin films deposited at different potentials.

The deduced data from these two figures (Fig. 3.13 and 3.14) in addition to calculated electrochromic parameters are tabulated in table (3.4).

As may observed from table (3.4), best electrochromic properties (highest contrast ratio (3.5), highest reversibility (0.88), highest coloration efficiency (14.81), and highest coloration difference (T_b-T_c)) was observed for annealed films electrodeposited at -700 mV. As observed before for $Ni(OH)_2$ films, NiO films deposited at -800 mV and higher has not stable CA measurements and hence worse electrochromic properties.

Table (3.4): Deduced and calculated electrochromic parameters for films after annealing (NiO) deposited using different deposition potentials (mV).

V (mV)	Q_c (C/cm^2)	Q_a (C/cm^2)	T_b (%)	T_c (%)	t_b (sec.)	t_c (sec.)	Reversibility(Q_c/Q_a)	T_b/T_c	CE (cm^2/C)
-1000-A	-	-	-	-	-	-	-	-	-
-800-A	9.34	9.22	63.2	51.7	7.9	8.8	1.01	1.22	9.3
-700-A	36.73	41.75	65.1	18.6	11.0	5.9	0.88	3.50	14.8
-600-A	27.37	35.60	88.8	54.7	7.9	4.90	0.77	1.62	7.7
-500-A	24.73	34.42	86.3	62.2	10.8	6.9	0.72	1.39	5.8

Comparing between non-annealed films ($Ni(OH)_2$ films) and post annealed films (NiO films), one can clearly see that post annealed films have better electrochromic parameters. From tables (3.1 and 3.4), at given electrodeposition potential, table (3.4) generally shows higher contrast ratio (T_b/T_c), higher charge reversibility (Q_c/Q_a) and higher coloration efficiency (CE). This enhancement of electrochromic parameters is due to the annealing of the films at 300 °C which enhances the crystallization of the film. Films will crystallize from the amorphous $Ni(OH)_2$ to crystallize NiO [82]. Crystalline films are known to have higher grain size and less grain boundary than amorphous. This indeed will enhance ion transport during electrochromic process. In addition, temperature ensure better homogeneity

of the film due to enhancing diffusion coefficient of the deposited layer which give higher adhesion and higher film uniformity. Hence post annealing enhances electrochromic parameters as observed for annealed films at 300 ˚C for one hour under air in comparison with non-annealed ones [83].

Better ion transport in post annealed films was confirmed by cyclic voltammogram (CV) measurements (Fig. 3.15), that performed for films before and after annealing and deposited at -700 mV potential. CV measurements for prepared films was done in 3-electrode electrochemical cell. 0.5 M KOH electrolyte was used in the cell with reference Ag/AgCl electrode.

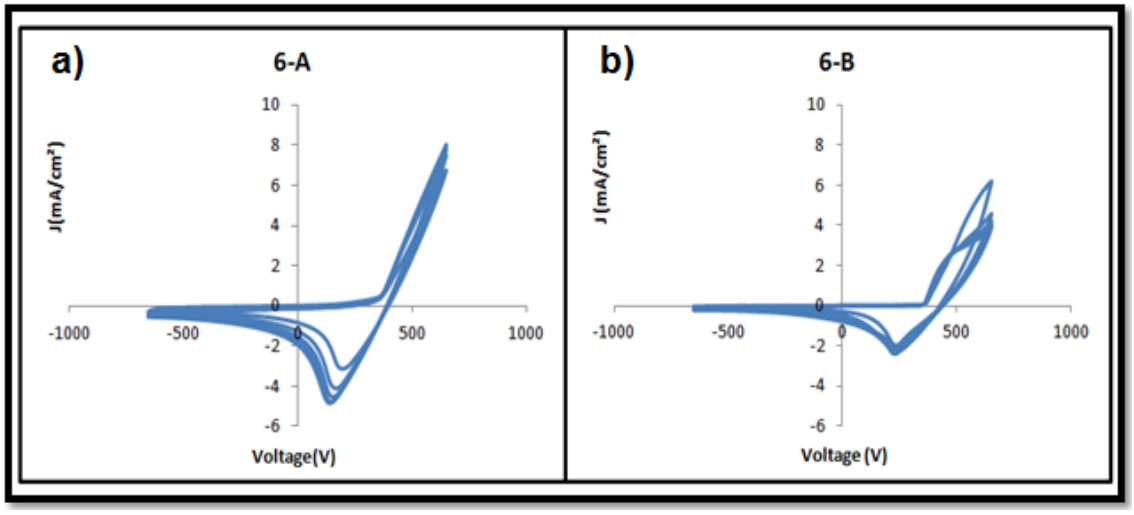


Figure (3.15): Cyclic voltammetry measurments for Ni-based thin films: a) NiO thin film annealing at 300 ˚C (A- after annealing) and b) as deposited film $Ni(OH)_2$ (B: before annealing).

$Ni(OH)_2$ or NiO electrochromic film deposited at -700 mV at one molar concentration was used in the cell as a working electrode. The scan rate of

the CV is 50 mV/s cycled between -650 mV to 650 mV. Higher anodic current (J_a) and cathodic current (J_C) peaks were observed (Fig. 3.15) for films post annealed at 300 °C for one hour under air. This confirms that post annealed film (NiO) have higher ionic diffusion coefficient than that not annealed film ($Ni(OH)_2$). The diffusion coefficient has direct relation with peak currents as shown in the following Randell-Sevcick formula:

$$i_p = 2.72 \times 10^5 \times n^{2/3} \times D^{1/2} \times C_o \times v^{1/2} \qquad (3.9)$$

where i_p is given peak current, D is the diffusion coefficient, n is number of electrons transferred per atom (assumed to be 1), v is the scan rate and C_o is concentration of active ions in the electrolyte. For as prepared films before annealing, $Ni(OH)_2$ films in CV measurements as shown in figure (3.15.a) have D_A of 7.78×10^{-13} cm^2/s and D_c of 1.35×10^{-13} cm^2/s that were calculated according to formula (3.9). On the other hand, post annealed films (NiO films) as shown in figure (3.15.b) have higher diffusion coefficient with D_A of 1.38×10^{-12} cm^2/s and D_c of 5.4×10^{-13} cm^2/s.

3.2.2.2 NiO optical parameters

For NiO prepared thin, the transparency for light wavelength ranges from 200-1000 nm is presented in (Fig. 3.16).

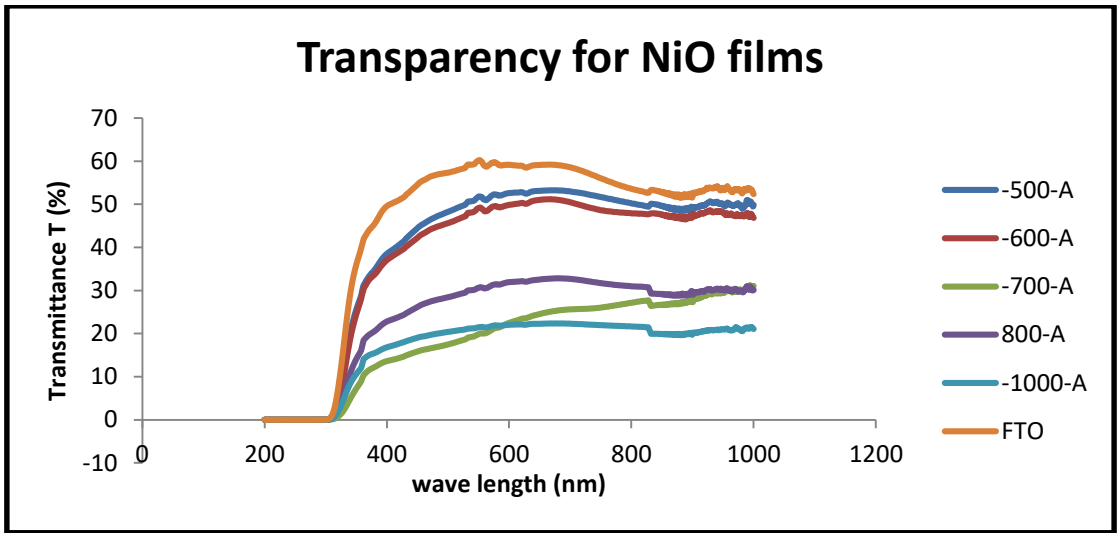


Figure (3.16): Transparency spectra for NiO films prepared at different deposition potentials.

As shown in figure (3.16), the transparency in the visible and near infrared of the films was found to have lower transmittance value compared with FTO/Glass substrate. this is expected since the films had brown color after annealing at 300 ºC. The brown color may be due to transformation of the film to NiOOH during annealing in air. During annealing, formed NiO grain surface may thermally oxidized from Ni^{2+} to Ni^{3+} forming NiOOH, which is the electrochromic color state for NiO transparent films [48, 56]. As also observed in figure (3.16), the transparency was found to decrease with increasing deposition potential. this as previously described due to increase in defect density introduced in the film when increasing the deposition potential. The high decrease in visible range transparency, for films deposited at -700 mV, may be attributed to the high concentration of the phase NiOOH on the NiO formed grains surfaces [48]. Higher concentration of colored NiO grains is due to NiOOH formation at their grains surfaces will increase the number of NiO grains that may share in

the electrochromic reaction. This may be the reason for having the best electrochromic properties as shown before.

a) NiO thin film thickness calculations.

The transparency measurements have been used to calculate the thickness of the NiO films (as done previously for $Ni(OH)_2$ films). The calculated thickness for different films prepared from different deposition potentials are presented in table (3.5).

Table (3.5): Calculated thickness for NiO films prepared using different deposition potentials.

Deposition potential	Thickness (nm)
-1000 mV-A	658
-800 mV-A	707
-700 mV-A	679
-600 mV-A	723
-500 mV-A	700

As expected, all films have almost the same thickness since all of them have same charge deposited on the same area. the slight change in the thickness may be due to slight difference in their density during annealing and/or due to calculation error margin.

b) NiO optical band gap determination

For different films, thickness (table 3.5) and absorption coefficient (α) calculated from transparency spectra of figure (3.16) was used to plot $(\alpha hv)^2$ versus hv (Fig. 3.17) assuming direct allowed transition for NiO [81].

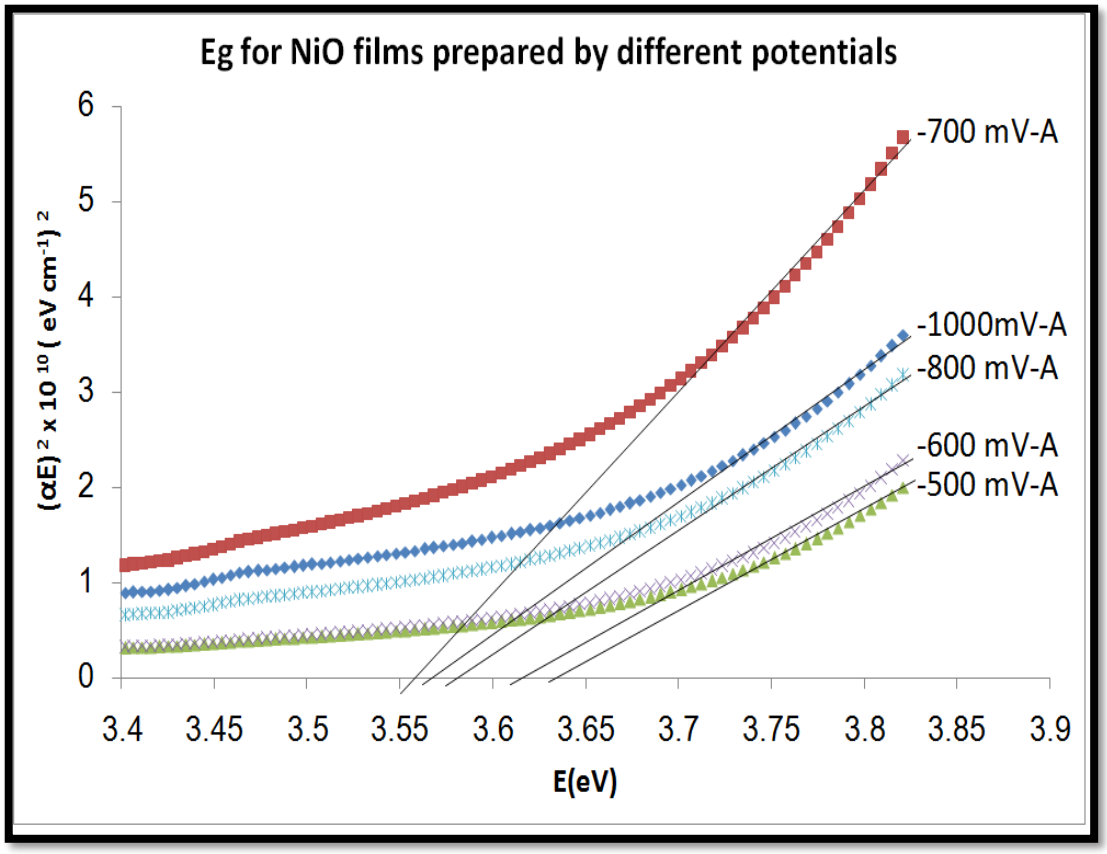


Figure (3.17): The plot of $(\alpha E)^2$ as a function of E for NiO films prepared using different deposition potentials**.**

The optical band gap (E_g) deduced from extrapolation of linear part of the plot (Fig. 3.17) are tabulated in table (3.6). The optical band gap for films deposited at different deposition potentials are recorded in table (3.6).

Table 3.6: The optical band gap for $Ni(OH)_2$ films deposited at different potentials.

NiO Deposition potential	E_g (eV)
-500-A	3.63
-600-A	3.62
-700-A	3.56
-800-A	3.58
-1000-A	3.57

From table (3.6), E_g for all films was found to have a value around 3.6 eV. The slightly difference in Eg (reduction) for potentials of -700 mV and

higher may be due to (as discussed before in (3.2.1.4-b)) increase in particle speed, that introduced defects in the film structure. Moreover, at higher potentials, NiOOH formation on the film increases, hence lowering the Eg (see discussion on linear sweep voltamogram (Fig. 3.10)). Also, all films have an optical band gap above 3.2 eV indicating that films are transparent in the visible rang.

3.3 Optimization of nickel nitrate molar concentration for Ni-based thin films electrodeposition.

Ni-based thin films were deposited, onto cleaned FTO/glass substrates, using different molar concentration of nickel nitrate hexahydrate ($Ni(NO_3)_2.6H_2O$) in the preparation solution. The concentrations used were 0.1, 0.3, 0.5, 0.8, and 1M. For all films, a total charge of -5 C were deposited onto (2×1 cm^2) substrate at optimized potential of -700 mV.

3.3.1 $Ni(OH)_2$ electrochromic films

As quoted before, $Ni(OH)_2$ thin films, prepared using different molar concentration of nickel nitrate, can be obtained by electrodeposition without annealing of the films (B-films). For these films different experiments have been performed; chronoamperometry (CA), transparency during CA, and transparency at variable wave length.

3.3.1.1 Molar concentration effect on $Ni(OH)_2$ electrochromic parameters

For $Ni(OH)_2$ films, CA and transparency experiments have been done to investigate different electrochromic and optical properties. CA and Transparency during CA measurements for $Ni(OH)_2$ films are shown in figures 3.18 and 3.19, respectively.

For different films prepared from different ($Ni(OH)_2$) concentrations, twenty chronoamperometry cycles (Fig. 3.18) was done of as deposited films ($Ni(OH)_2$) in 0.5 M KOH. The potential was cycled between -650 mV and 650 mV versus Ag/AgCl reference electrode. Each cycle potential was kept for duration of 20 s. In addition, transparency during CA (Fig. 3.19) was also done for these films. The transparency during CA actualized at light wavelength of 630 nm because deeper and faster response of NiO [84].

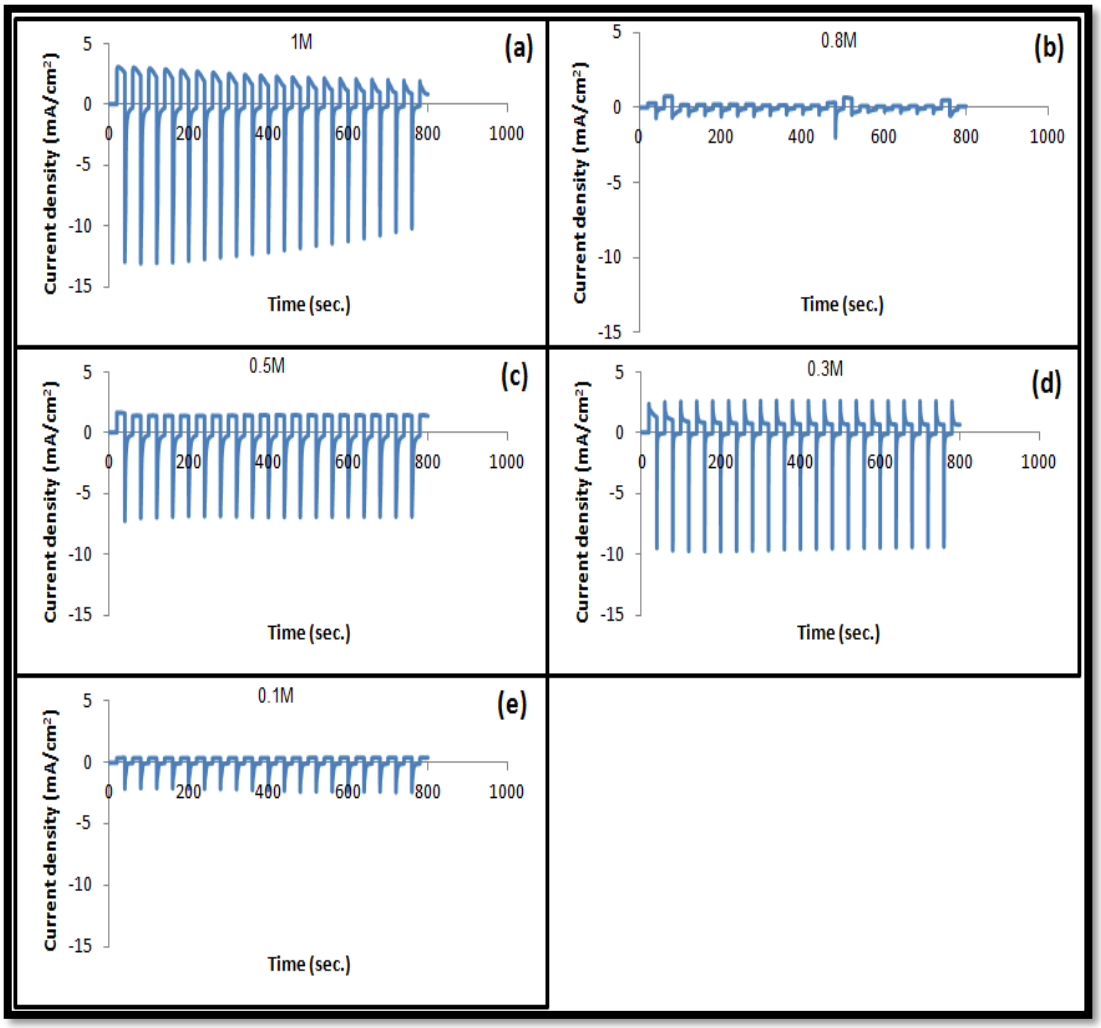


Figure (3.18): Twenty CA cycles $Ni(OH)_2$ thin films prepared using different molar concentrations of $Ni(NO_3)_2.6H_2O$ potential cycled between -650 mV and 650 mV versus Ag/AgCl reference electrode in 0.5M KOH.

As shown in figure (3.18), films deposited at molar concentrations 0.1, 0.5 and 0.8 M shows unusual anodic current density (J_a) behavior. Constant current was observed at given anodic potential during cycling. This indicate that the film does not totally covers the substrate. The constant current indicates that the resistance is constant during charge intercalation. Indeed, this is due to the resistance of conductive FTO/class substrate which seems to be in contact with the KOH electrolyte; the $Ni(OH)_2$ film didn't totally

cover the FTO layer. Other films deposited at 1 and 0.3 M generally shows almost a normal and stable anodic and cathodic current density response upon charge intercalation. Note that the current density for 1M concentration becomes more stable as cycle number increase. This is because the coloration sites sharing the electrochromic reaction are not yet saturated and become close to saturation upon cycling; stability of current density indicate that number of charges inserted per unit area is stable, hence no more area is affected by more or less charge intercalation.

CA measurements, as described in the previous parts, are used to find anodic charge density (Q_a), cathodic charge density (Q_c), bleaching time (t_b), and coloration time (t_c). The deduced quantities (Q_a, Q_c, t_c, and t_b) at cycle 20 are shown in table (3.7) below.

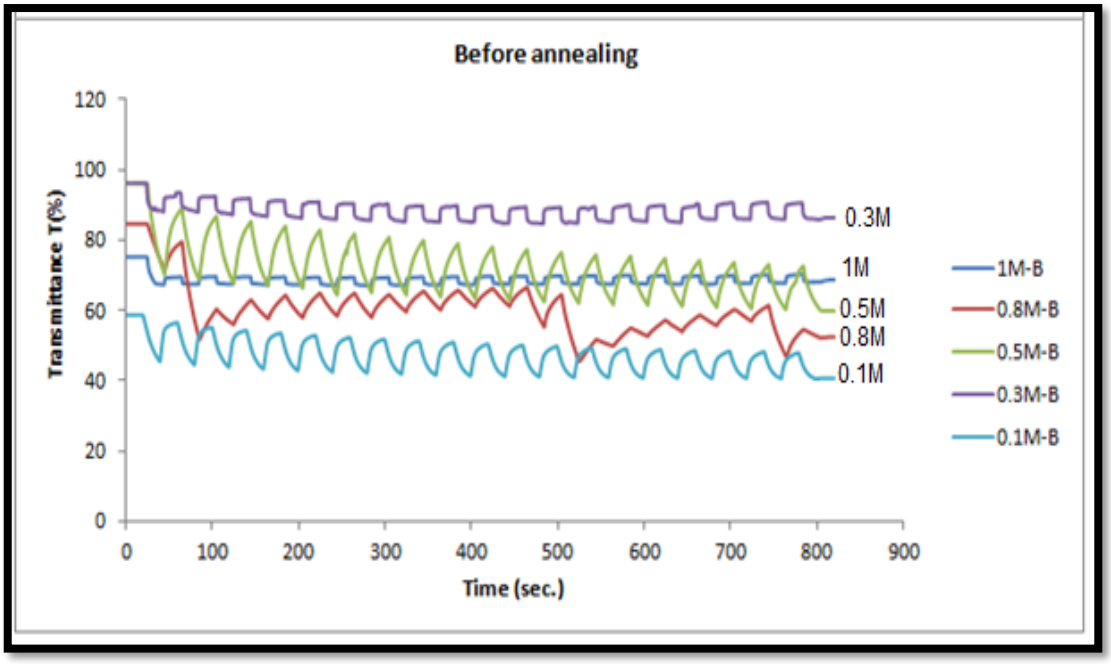


Figure (3.19): Optical transmittance change at 630 nm wave length of Ni(OH)2 thin films deposited using different molar concentration of Ni(NO3)2.6H2O.

Transparency during CA (Fig. 3.19) shows a weak coloration bleaching response for all films. This is due to the fact that these films may not totally cover the substrate and the conductive substrate shares in the current densities; shown current density is a result of current transport from the film and FTO substrate at the solid-liquid interface. Hence poor coloration bleaching difference is observed. From transparency measurements of prepared films, T_c and T_b are found for cycle 20 and tabulate in table (3.7). The data collected in table (3.7) were used to calculate different electrochromic parameters, reversibility, contrast ratio (T_b/T_c), and coloration efficiency (C.E). These calculated parameters are tabulated also in table (3.7).

Table (3.7): Deduced and calculated electrochromic parameters for films before annealing ($Ni(OH)_2$) deposited from different $Ni(NO_3)_2.6H_2O$ molar concentrations.

$Ni(NO_3)_2$ conc.	Q_c (C/cm^2)	Q_a (C/cm^2)	T_b (%)	T_c (%)	t_b (sec)	t_c (sec)	Reversibility (Q_c/Q_a)	T_b/T_c	CE (cm^2/C)
0.1M-B	7.10	8.10	48.4	40.7	9.8	11.0	0.88	1.19	10.6
0.3M-B	8.41	16.51	91.2	85.8	6.9	7.8	0.51	1.06	3.0
0.5M-B	25.33	27.27	73.3	59.5	6.9	6.9	0.93	1.23	3.6
0.8M-B	5.74	9.79	54.9	47.0	11.8	11.8	0.60	1.17	11.9
1M-B	1.29	6.92	71.6	68.2	2.9	05.9	0.19	1.05	16.4

From table (3.7), some calculated electrochromic parameters like coloration efficiency and reversibility have good high values. But

unfortunately, T_b/T_c for all concentrations was found to be around one due to low coloration bleaching transparency difference. This indicates a poor electrochromic performance for these films when deposited at -700 mV before annealing.

3.3.2 Molar concentration effect on NiO electrochromic films

$Ni(OH)_2$ films prepared from different $Ni(NO_3)_2.6H_2O$ were annealed at 300 °C. As mentioned before, annealing $Ni(OH)_2$ films will transform them to NiO thin films.

3.3.2.1 NiO Electrochromic properties

CA (Fig. 3.20) and transparency during CA (Fig. 3.21) experiments have been done for NiO films, prepared using different $Ni(NO_3)_2.6H_2O$ molar concentrations.

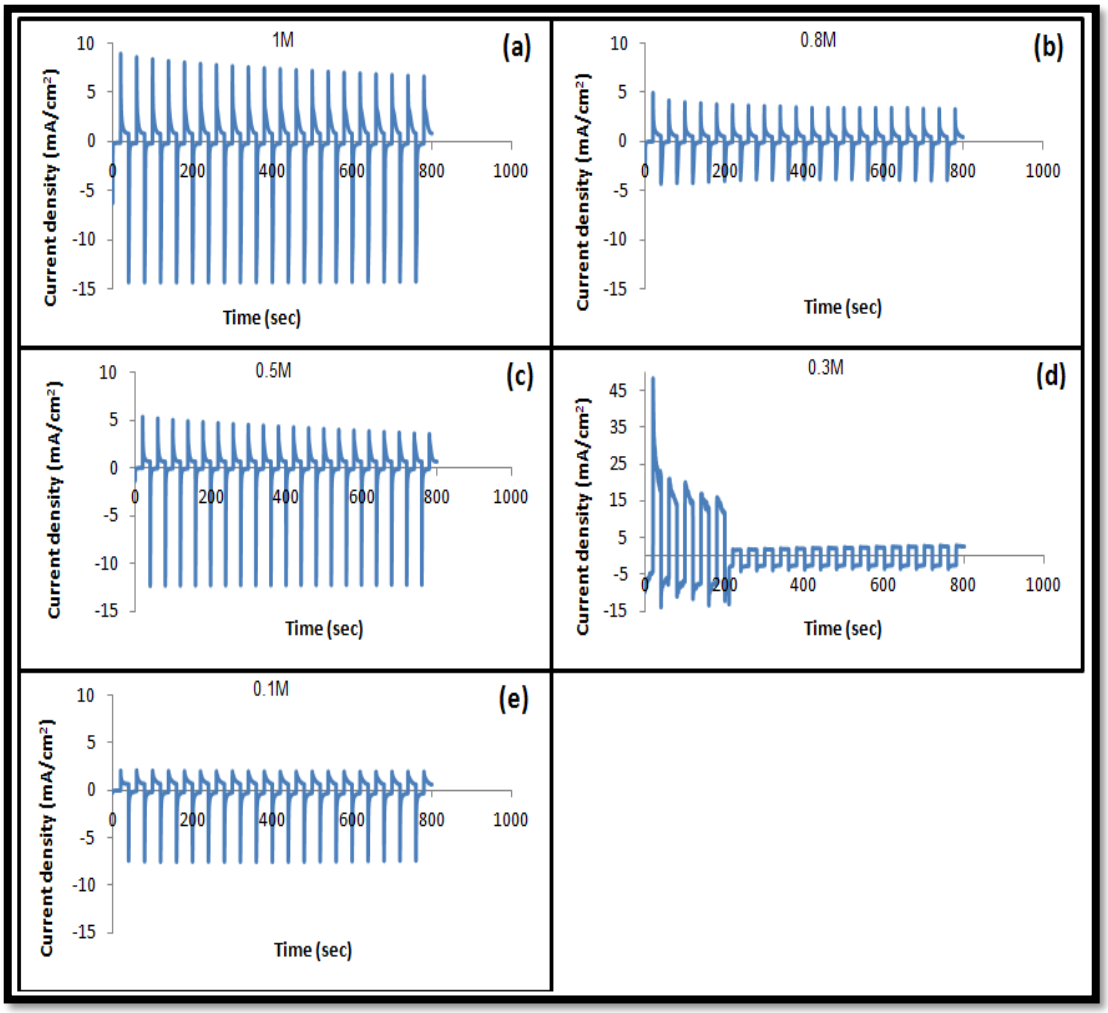


Figure (3.20): Twenty cycles CA curves for NiO films (A-films) prepared using different molar concentration of Ni(NO3)2.6H2O. The potential cycled between -650 mV and 650 mV versus Ag/AgCl reference electrode in 0.5 M KOH electrolyte.

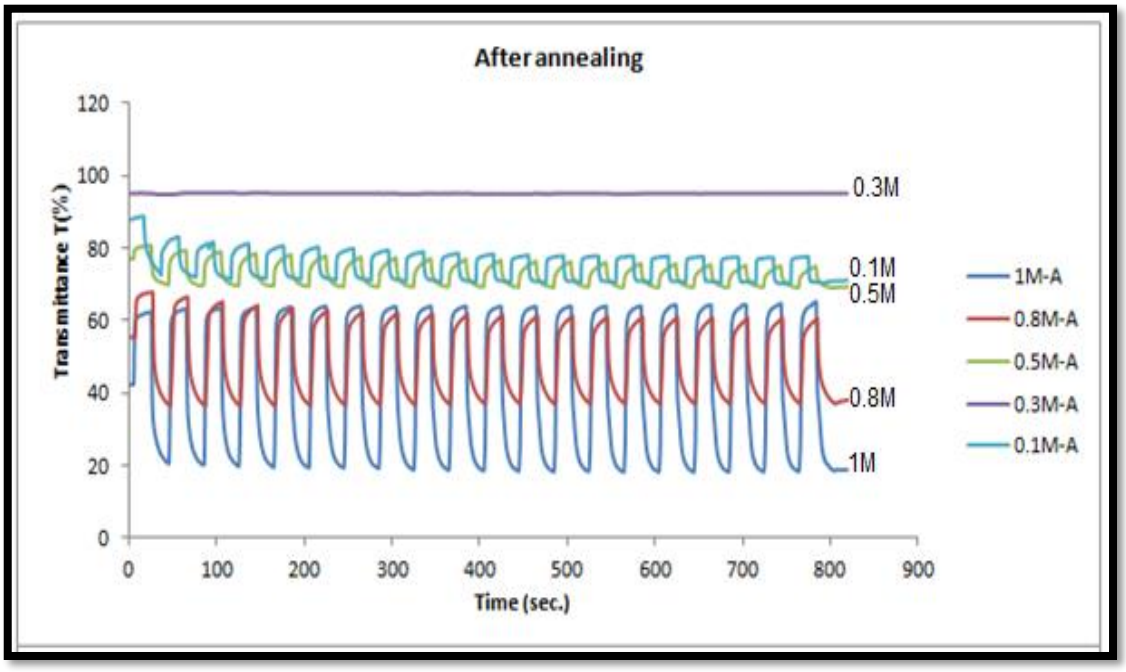


Figure (3.21): Optical transmittance change at 630 nm wave length during CA for NiO thin films deposited using different concentrations of $Ni(NO_3)_2.6H_2O$.

Typical CA graphs (Fig 3.20) are observed for all films except the film prepared from 0.3 M concentration. The film shows a constant current density upon cycling; after cycle number 5. After cycle numbers, the film was observed to wear out in the cell. This means the film wears out and the substrate becomes in contact with the electrolyte.

Transparency during CA (Fig. 3.21) shows, as expected, no coloration bleaching for film deposited at 0.3M. Also, figure (3.21) shows a poor coloration bleaching transparency change for films prepared from 0.1 and 0.5M concentrations. On the other hand, film deposited from 0.8 and 1M concentrations shows a pronounced coloration bleaching transparency difference. The coloration bleaching transparency difference is observed to be the highest for films prepared from 1M concentration of

$Ni(NO_3)_2.6H_2O$. Hence, this film is expected to have best electrochromic parameters.

Figures (3.20 and 3.21) was used to calculate different electrochromic parameters using different quantities obtained from these Figures (Q_a, Q_c, T_b, and T_c). Table (3.8) shows deduced electrochromic parameters from CA and from transparency during CA in addition to calculated electrochromic parameters.

Table (3.8): Deduced and calculated electrochromic parameters for films after annealing (NiO) deposited from different $Ni(NO_3)_2.6H_2O$ molar concentrations.

$Ni(NO_3)_2$ conc.	Q_c (C/cm^2)	Q_a (C/cm^2)	T_b (%)	T_c (%)	t_b (sec)	t_c (sec)	Reversibility (Q_c/Q_a)	T_b/T_c	CE (cm^2/C)
0.1 M-A	15.43	18.95	77.5	70.0	8.8	8.8	0.81	1.11	2.9
0.3 M-A	52.00	51.77	-	-	8.8	7.8	0.99	-	-
0.5 M-A	17.74	23.99	75	68.4	8.8	5.9	0.74	1.10	2.3
0.8 M-A	13.68	15.20	60.7	36.6	6.9	6.9	0.90	1.66	16.1
1 M-A	36.73	41.75	65.1	18.6	10.8	5.9	0.88	3.50	14.8

As observe from table (3.8), highest coloration efficiency (16.1) and good reversibility (0.90) were for films deposited from 0.8 M of $Ni(NO_3)_2.6H_2O$. However, it's contrast ration (T_b/T_c = 1.66) is low compared to films prepared from 1M which have a contrast ratio of 3.5. This is due to highest coloration bleaching transparency difference. On the other hand, coloration efficiency and reversibility for 1M are close to those of 0.8M. Hence, the films prepared from 1 M of $Ni(NO_3)_2.6H_2O$ are considered to be almost the best from the electrochromic parameters point of view.

Comparing between non-annealed films ($Ni(OH)_2$) and post annealed films (NiO) (table (3.7 and 3.8)) , post annealed films generally show better electrochromic parameters, especially for films deposited from 0.8 M and 1M of $Ni(NO_3)_2.6H_2O$ in term of contrast ratio (T_b/T_c), highest contrast ratio at given electrodepostion molarity, table (3.8) in general shows high charge reversibility (Q_c/Q_a), higher coloration efficiency, and higher contrast ratio (T_b/T_c). one can clearly see that post annealed films have in general best electrochromic parameters. This is due to better diffusion of the film leading to full coverage to the substrate. Hence no linear current density was observed (Fig. 3.20) and the current is only from the film exposed to electrolyte. In addition, better contrast ratio observed, when increasing molar concentration used in the preparation, may be due to formation of higher density of NiOOH phase on the NiO grains surfaces during annealing of the films.

3.3.2.2. Molar concentration effect on NiO optical parameters

As done for previous films, transparency measurements (Fig. 3.22) of NiO thin films have been performed for light wavelength ranges from 200-1000 nm.

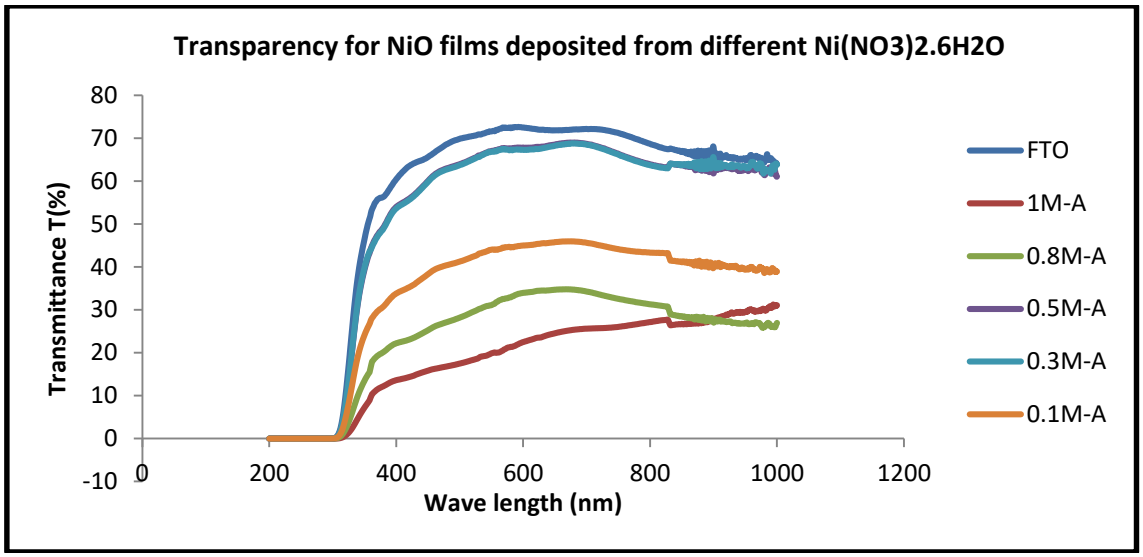


Figure (3.22): Transparency spectra for NiO films prepared from different $Ni(NO_3)_2.6H_2O$ concentrations.

Figure (3.22) shows that the transparency in the visible and near infrared of the films which was found to have lower transparency compared with FTO/Glass substrate. As described before, this is due to brown color arise thermally formed NiOOH phase [48, 54]. Films prepared from 0.8 and 1M of $Ni(NO_3)_2.6H_2O$ had the lowest transparency due to higher concentration of NiOOH phase in these films. Hence, these films had best electrochromic properties as shown before.

a) Molar concentration effect on NiO thin film thickness calculations

As done before, thickness of the NiO films were calculated from interference fringes of transparency measurements. The calculated thickness for different films prepared from different deposition potentials are presented in table (3.9).

Table (3.9): Calculated thickness for NiO films prepared using molar concentration of $Ni(NO_3)_2.6H_2O$.

$Ni(NO_3)_2.6H_2O$ concentration	**Thickness (nm)**
0.1 M	757
0.3 M	672
0.5 M	672
0.8 M	757
1.0 M	679

As for previous films, since all films have same charge deposited on same area, all films have almost the same thickness. The change in the thickness is (as quoted before) may be due to difference in their density during annealing and/or due to calculation error margin.

b) Molar concentration effect on NiO optical band gap determination

Assuming direct allowed transition [81], a plots of $(\alpha hv)^2$ versus hv for NiO thin films (Fig. 3.23) have been done to extrapolate linear part of the plots and find the films optical band gaps (E_g). Indeed, we have used films thickness (table 3.9) and transparency measurements (Fig. 3.22) to calculate absorption coefficient (α), as done before.

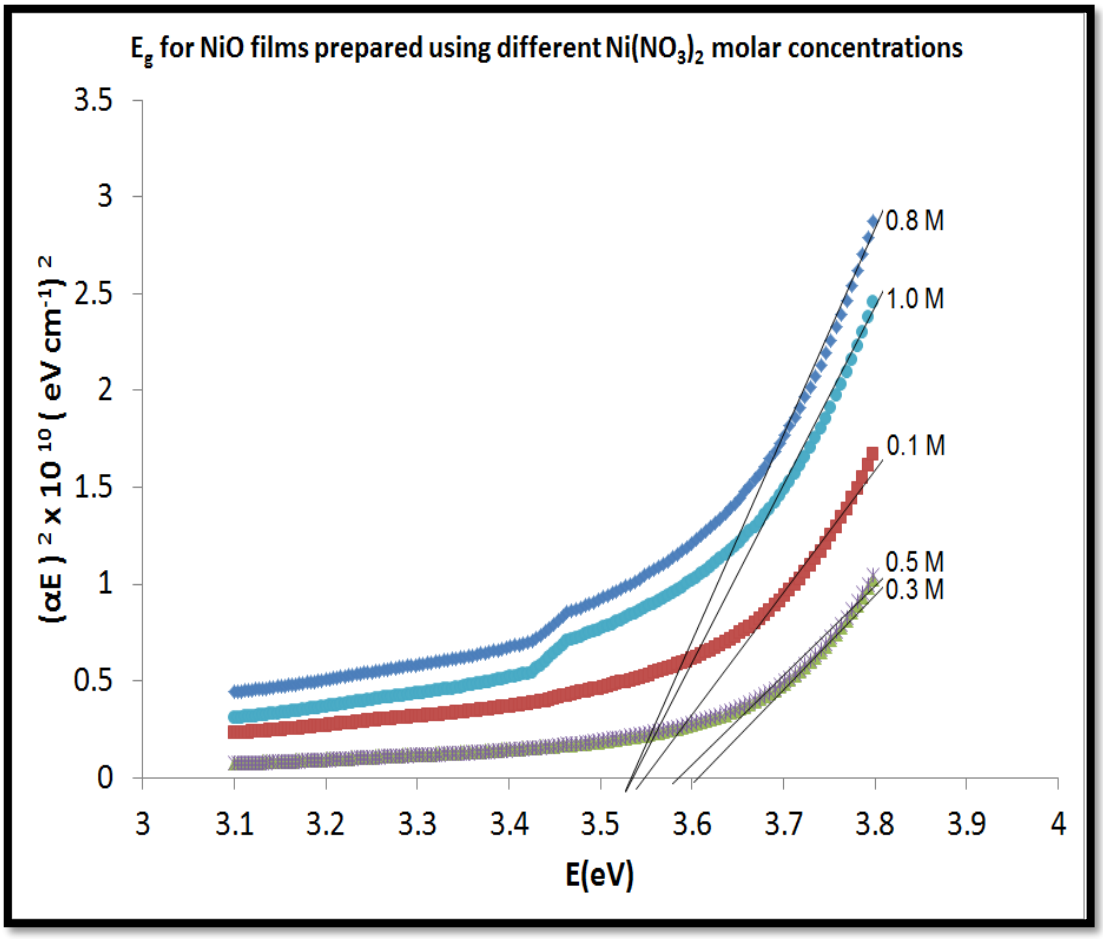


Figure (3.23): The plot of (αE)2 as a function of E for NiO films prepared using different Ni(NO3)2.6H2O molar concentration.

For films deposited using different $Ni(NO_3)_2.6H_2O$ molar concentration, the deduced E_g from the plots (Fig. 3.23) are tabulated in table (3.10).

Table (3.10): The optical band gap for NiO films deposited at different potentials.

$Ni(NO_3)_2.6H_2O$ concentration	**E_g (eV)**
0.1 M	3.55
0.3 M	3.61
0.5 M	3.58
0.8 M	3.53
1.0 M	3.53

From table (3.6), E_g was found increase when increasing the $Ni(NO_3)_2.6H_2O$ concentration up to 0.3 M. however, E_g decrease for concentrations of 0.5 M or higher. This change in E_g, again, may be related to the concentration of NiOOH in the thin film when annealed at 300 ºC and to the grain size that increase with increasing $Ni(NO_3)_2.6H_2O$ concentration. Indeed, as molar concentration increase, the current density of the electrodeposition increase and hence introducing higher defect density in addition to higher agglomerated particles with higher size [23]. this results in decreasing the optical band gap as shown in the table above.

3.3.2.3 Structural properties

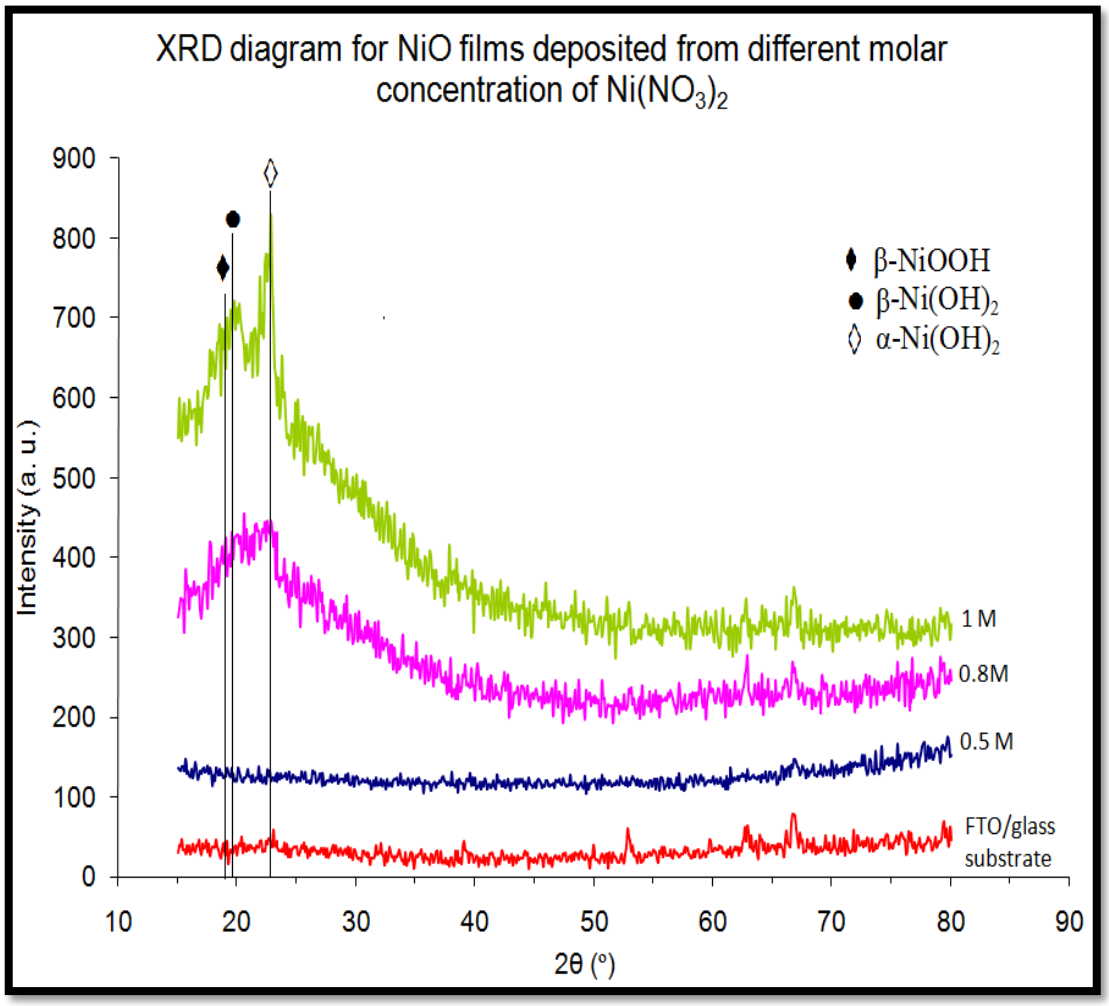


Figure (3.24): Schematic shows XRD for NiO films deposited from different molar concentration of Ni(NO3)2.6H2O.

XRD measurements (Fig. 24) have been done for annealed (at 300 ºC for 1 hour) films prepared from different molar concentration of $Ni(NO_3)_2.6H_2O$. XRD measurements shows a polymorphous nano structure films. The film deposited from 0.5 M has no peaks correspond to Ni compounds. This reveals the amorphous nature of the film. On the other hand, for films deposited from 0.8 M and 1 M, XRD diagram confirms the existence of the phases α-$Ni(OH)_2$ (JCPDS: 38-715), β-$Ni(OH)_2$ (JCPDS: 14-117), and β-

NiOOH [85]. Other observed weak peaks are corresponded to the FTO/glass substrate (the FTO XRD diagram is added to figure 24 as a reference). As observed for other works [86], both phases of $Ni(OH)_2$ exist, since as deposited films reaction produces $Ni(OH)_2$ phases. After annealing, part of Ni^{2+} ($Ni(OH)_2$) phases will be oxidized to Ni^{3+} (β-NiOOH) phase as confirmed by XRD diagram above. Also, the observed XRD results indicates that as the concentration of $Ni(NO_3)_2.6H_2O$ increases in the deposition solution, the crystallinity enhances; amorphous film for 0.5 M, crystalline film with crystallite size of 2 nm for 0.8 M, and crystalline film with crystallite size of 12 nm for 1 M. Moreover, the intensity of the peaks (particularly NiOOH) increases with increasing molar concentration of $Ni(NO_3)_2.6H_2O$. This indicate higher concentration of NiOOH (colored state of NiO) in the film deposited from 1M of $Ni(NO_3)_2.6H_2O$. Indeed, higher coloration sites will lead to higher coloration of the film in the color state and hence, better electrochromic parameters under coloration bleaching process.

3.3.2.4 Cycling stability

From previous experiments, done for different deposition potentials and different $Ni(NO_3)_2.6H_2O$ molar concentrations, we could optimize best deposition conditions for best NiO electrochromic film. The best electrochromic NiO film that was prepared from 1 M of $Ni(NO_3)_2.6H_2O$, deposited at -700 mV, and finally annealed at 300 ºC.

For this film, CA measurements was done for 400 cycles to evaluate its stability. CA was done during transparency measurements at light wavelength of 630 nm. The potential was cycled, versus Ag/AgCl reference electrode, between -650 and 650 mV in 0.5 M KOH solution. CA and Transparency during CA for cycles number 2, 200, and 400 are shown in figure (3.24) and figure (3.25), respectively.

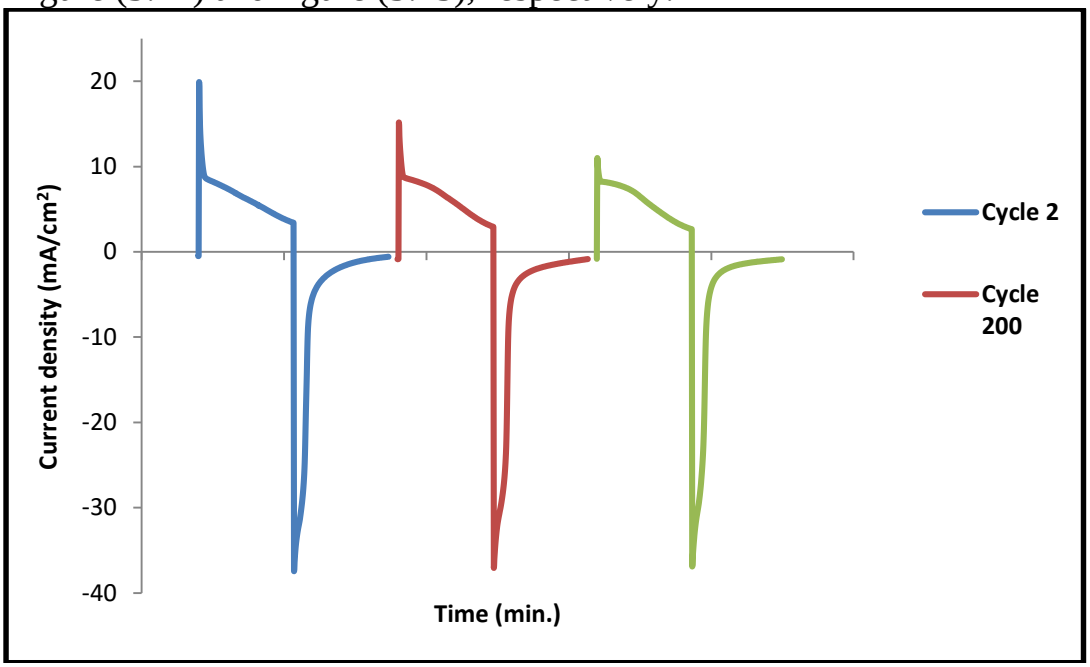


Figure (3.25): CA curve for cycles 2, 200, and 400 of electrochromic NiO film prepared at optimal conditions (1 M $Ni(NO_3)_2.6H_2O$, -700 mV deposition potential, and annealed at 300 ºC).

Good CV curves was obtained for the 400 cycles as shown in figure (3.25). upon cycling the anodic current density peak decrease and the cathodic current density remained the same but becomes narrower. This indicates that with increasing cycle number, lower charge densities (see table 3.11) is intercalated during coloration bleaching process. On the other hand, transparency during CA (Fig. 3.26) was found to have higher coloration

bleaching transparency difference. This means an increase in the coloration sites sharing the electrochromic process upon cycling. This is due to the fact that electrochromic activity initiating in a thin interface layer covering the NiO grains grows with cycling till reaching the full depth of the covering layer [37]. Unfortunately, we didn't reach the full depth because the calculated electrochromic parameters (table 3.11) is still enhancing while increasing cycle number and we didn't observe where it decreases.

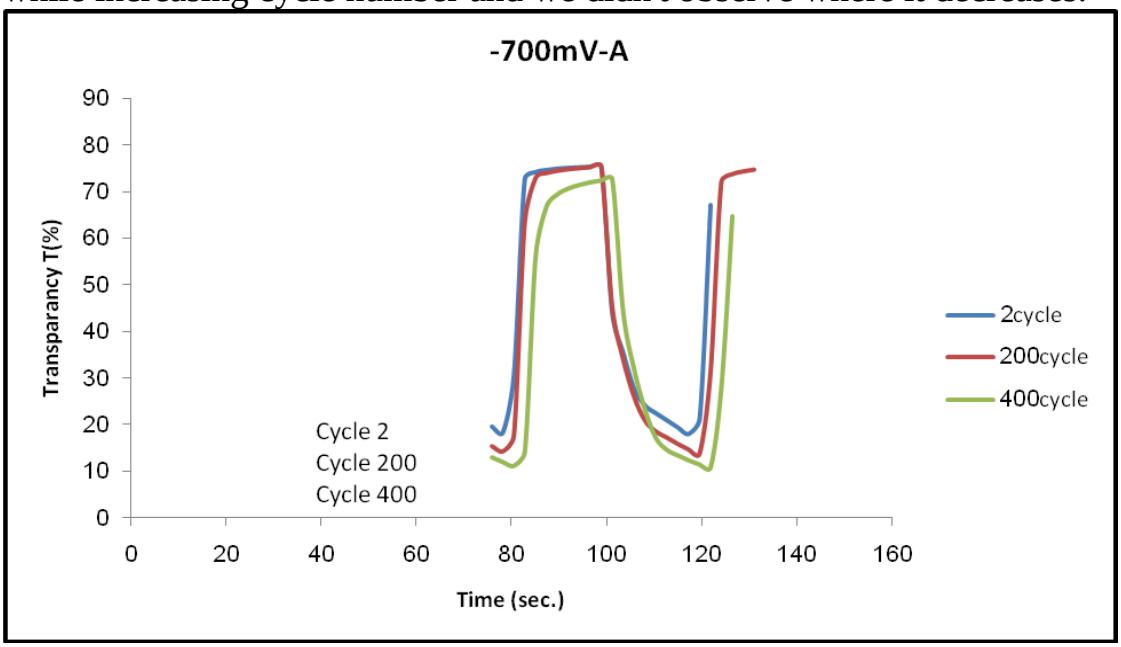


Figure (3.26): Optical transmittance change at 630 nm wave length of NiO thin films with voltages -700 mV after annealing at 300 ˚C for one houre under air at molar concentration 1M.

The deduced data from these two figures (Fig. 3.25 and 3.26) in addition to calculate electrochromic parameters are tabulated in table (3.11).

Table (3.11): Deduced and calculated electrochromic parameters for cycle number 2, 200, 400 of NiO thin film prepared at optimum conditions (-700 mV deposition potential, 1M $Ni(NO_3)_2.6H_2O$, and annealed at 300 ºC).

Cycle number	Q_a (C/cm^2)	Q_c (C/cm^2)	T_b (%)	T_c (%)	T_b/T_c	Reversibility (Q_c/Q_a)	CE (cm^2/C)
2	63.18	59	75.47	18.11	4.17	0.93	10.50
200	62.83	60.85	75.44	13.65	5.53	0.97	12.20
400	57.70	55.85	72.63	10.71	6.79	0.97	14.89

As it is observed from table (3.11), best electrochromic properties (highest contrast ratio (6.79), highest reversibility (0.97), and highest coloration efficiency (14.89)) was observed at cycle No. 400 for annealed film of 1M concentration electrodeposited at -700 mV, and 300 °C.

3.4 General conclusions

Deposition of Ni-based thin films on (FTO/glass) substrate was done by electrodeposition technique. The nickel-based films were prepared by adding certain molar concentration (from 0.1 M to 1 M) of nickel nitrate hexahydrate ($Ni(NO_3)_2.6H_2O$) with 25 ml of distilled water. The mixture were stirred by a magnet for 20 minutes at room temperature. Then the film was deposited on the FTO/glass substrate by electrodeposition at different deposition potentials (from -500 mV to -1000 mV). Finally, the deposited films were heated at 300 °C for one hour under air.

In order to optimize best preparation conditions for different Ni-based electrochromic films, different preparation parameters have been studied. First, we have studied the effect of different cleaning methods on films homogeneity and adhesion to substrate. After that, effect of different deposition potentials on optical and electrochromic properties were studied for as deposited and post annealed films. Then, for as deposited and post annealed films, we have studied the optical and electrochromic properties for films prepared using different $Ni(NO_3)_2.6H_2O$ molar concentration. In addition, structural properties using XRD measurements were studied for post annealed films, prepared from different molar concentrations of $Ni(NO_3)_2.6H_2O$. Finally, we have done stability measurements up to 400 coloration bleaching cycles for film of optimized preparation conditions.

In order to deposit a homogeneous, and good adhesion films, seven different cleaning methods of the (FTO/glass) substrate was done. The sixth cleaning process was found to be the best one of them, since it gave the best homogeneity and adhesion of NiO thin film with the (FTO/glass) substrate. The sixth method was cleaning the films using dish washing liquid soap followed by successive immersion of substrates into sonicated isopropanol, aceton and ethanol. These films were soacked in diluted HCL, before finally rinsed with deionized water and dried at 100 ^{o}C.

Depending on the best method of cleaning methods (sixth cleaning method) to (FTO/glass) substrate. The second parameter is to choose the best potential value of NiO thin films - that have the same thickness - from different deposition potentials (-500, -600, -700, -800 and -1000 mV) at the

same molar concentration of 1M. The potential that gave electrochromic annealed films with higher values of electrochromic parameters (coloration efficiency (14.8 cm^2 /C), reversibility (0.88) and contrast ratio (3.50)) was the -700 mV.

After the best potential (-700 mV) was known, the third parameter is to find the suitable molar concentration value of $Ni(NO_3)_2.6H_2O$. different molar concentrations (0.1, 0.3, 0.5, 0.8 and 1 M) were used of in the preparation solution. The molar concentration of 1 M was selected since the obtained annealed electrochromic film had the best value of electrochromic parameters (reversibility (0.88), coloration efficiency (14.8 cm^2 /C) and contrast ratio (3.5)).

In summary, best electrochromic film that gives highest electrochromic performance can be obtained by cleaning the substrate using sixth cleaning method before film deposition. After that depositing the film by electrodeposition using a potential of -700 mV in a solution that contains 1 M of $Ni(NO_3)_2.6H_2O$. then annealing the film at 300 °C for 1 hour under air. This film shows a high stability and increasing in the electrochromic performance up to 400 coloration bleaching cycles. In addition, it shows a nanocrystal structure of crystallite size of 12 nm as shown from XRD diagram.

References

[1] F.F. Ferreira, M.H. Tabacniks, M.C.A. Fantini, I.C. Faria and A. Gorenstein, ***"Electrochromic nickel oxide thin films deposited under different sputtering conditions"*** ASolid State Ionics, **86-88**:971-976, (1996).

[2] E. Fujii, A. Tomozawa, H. Torii, and R. Takayama, ***"Preferred orientations of NiO films prepared by plasma-enhanced metal organic chemical vapor deposition"*** Japanese Journal of Applied Physics, **35**(3): L328–L330, (1996).

[3] H.Sato, T. Minami, S. Takata, and T. Yamada, ***"Transparent conducting p-type NiO thin films prepared by magnetron sputtering"*** Thin Solid Films, **236**(1-2): 27-31, (1993).

[4] B. Sasi, K.G. Gopchandran, P.K. Manoj, P. Koshy, P. PrabhakaraRao, and V.K. Vaidyan, ***"Preparation of transparent and semiconducting NiO films"*** Vacuum, **68**(2): 149-154, (2003).

[5] K.S. Ahn, Y.C. Nah, and Y.E. Sung, ***"Surface morphological, microstructural, and electrochromic properties of short-range ordered and crystalline nickel oxide thin films"*** Applied Surface Science, **199**(1-4): 259-269, (2002).

[6] A.K. Roslik, V.N. Konev, and A.M. Maltsev, ***"The effect of surface condition and sulfur on the environmental resistance of airfoils"*** Oxidation of Metals, **43**(1):1-23, (1995).

[7] I.Fasaki, A. Giannoudakos, M. Stamataki, M. Kompitsas, E. György, I.N. Mihailescu, F. Roubani-Kalantzopoulou, A. Lagoyannis, and S.

Harissopulos, ***"Nickel oxide thin films synthesized by reactive pulsed laser deposition: characterization and application to hydrogen sensing"*** Applied Physics A, **91**(3):487-492, (2008).

[8] X. Chen, N.J. Wu, L. Smith, and A. Ignatiev, ***"Thin-film heterostructure solid oxide fuel cells"*** Applied Physical Letters, **84**(14): 2700-2702, (2004).

[9] Dler Adil Jameel[1, 2, *] **"Thin Film Deposition Processes"** International Journal of Modern Physics and Applications, **1**(4):193-199, (2015).

[10] J.-K. Kang, and S.W. Rhee, ***"Chemical vapor deposition of nickel oxide films from $Ni(C_5H_5)_2/O_2$"*** Thin Solid Films, **391**(1):57-61, (2001).

[11] J.D. Desai, S.K. Min, K.D. Jung, and O.S.Joo, ***"Spray pyrolytic synthesis of large area NiO_x thin films from aqueous nickel acetate solutions"*** Applied Surface Science, **253**(4):1781-1786, (2006).

[12] D.J. Taylor, P.F. Fleig, S.T. Schwab, and R.A. Page, ***"Sol–gel derived, nanostructured oxide lubricant coatings"*** Surface and Coatings Technology**, 120-121**:465-469, (1999).

[13] J.L. Garcia-Miquel, Q. Zhang, S.J. Allen, A. Rougier, A. Blyr, H.O. Davies, A.C. Jones, T.J. Leedham, P.A. William, and S.A.Impey, ***"Nickel oxide sol–gel films from nickel diacetate for electrochromic applications"*** Thin Solid Films, **424**(2):165-170, (2003).

[14] P. Pramanik, and S. Bhattacharya, ***"A chemical method for the deposition of nickel oxide thin films"*** Journal of the Electrochemical Society, **137**(12):3869-3870, (1990).

[15] S. Banerjee, A. Santhanam, A. Dhathathrenyan, and P.M. Rao, ***"Synthesis of ordered hexagonal mesostructured nickel oxide"*** Langmuir, **19**(13):5522-5525, (2003).

[16] K. Nakaoka, J. Ueyama, and K. Ogura, ***"Semiconductor and electrochromic properties of electrochemically deposited nickel oxide films"*** Journal of Electroanalytical Chemistry, **571**(1):93-99, (2004).

[17] J.W. Park, J.W. Park, D.Y. Kim, and J.K. Lee, ***"Reproducible resistive switching in nonstoichiometric nickel oxide films grown by rf reactive sputtering for resistive random access memory applications"*** Journal of Vacuum Science & Technology A, **23**:1309-1313, (2005).

[18] H.L. Chen, Y.M. Lu, and W.S. Hwang, ***"Thickness dependence of electrical and optical properties of sputtered Nickel oxide films"*** Thin Solid Films, **514**(1-2):361-365, (2005).

[19] K. S. Usha, R. Sivakumar, C. Sanjeeviraja, Vasant Sathe, V. Ganesand and T. Y. Wange, ***"Improved electrochromic performance of a radio frequency magnetron sputtered NiO thin film with high optical switching speed"*** RSC Advances, **6**(83):79668-79680, (2016).

[20] J. Velevska, M. Pecovska-Gjorgjevich, M. Najdoski and N. Stojanov, *" **Studies on electrochromism of chemically deposited nickel oxide thin films"*** Silpakorn U Science & Tech J, **5**(1):34-42, (2011).

[21] M. P. Browne, H. Nolan, N. C. Berner, G. S. Duesberg, P. E Colavita and M. E. G. Lyons, ***"Electrochromic nickel oxide films for smart window applications"*** Int. J. Electrochem. Sci.,**11:**6636 – 6647, (2016).

[22] K.J. Patel, C.J. Panchal, M.S Desai and P.K. Mehta***, "Optical and electrochromic properties of e-beam evaporated nickel oxide thin film"*** J. Nano- Electron. Phys.,**3**(1): 362-369, (2011).

[23] Vikas Patil1, Shailesh Pawar, Manik Chougule, Prasad Godse, Ratnakar Sakhare,Shashwati Sen, Pradeep Joshi, " **Effect of annealing on structural, morphological, electrical and optical studies of nickel oxide thin films"** Journal of Surface Engineered Materials and Advanced Technology, **1** : 35-41, (2011).

[24] A.C. Sonavanea, A.I. Inamdar, P.S. Shinde, H.P. Deshmukh, R.S. Patil and P.S. Patil, ***"Efficient electrochromic nickel oxide thin films by electrodeposition"*** Journal of Alloys and Compounds, **489**:667-673, (2010).

[25] Y. Akaltun, T. Cayır, ***"Fabrication and characterization of NiO thin films prepared by SILAR method"*** Journal of Alloys and Compounds, **625**: 144–148, (2015).

[26] T. Sen, R. Thangavel and U. G. Nair, ***"Study of morphological and electrical properties of zinc doped nickel oxide thin film prepared by***

facile sol-gel method" XXX International Conference on Surface Modification Technologies (SMT30), (2016).

[27] M. Vigneshkumar, S. Muthulakshmi @ Suganya, J. Pandiarajan, A. Saranya and N. Prithivikumaran, ***"Structural and optical properties of nanocrystalline nickel oxide thin film by spray pyrolysis technique"*** International Journal of Technical Research and Applications, (38):52-56, (2016).

[28] M. Guziewicz, J. Grochowski, M. Borysiewicz, E. Kaminska, J. Z. Domagala, W. Rzodkiewicz, S. Witkowski,K. Golaszewska, R. Kruszka, M. Ekielski and A. Piotrowska, *"**Electrical and optical properties of NiO films deposited by magnetron sputtering**"* Optica Applicata,**41**(2), (2011).

[29] V. Gowthami, M.Meenakshi, P. Perumal, R. Sivakumar and C. Sanjeeviraja, ***"Optical dispersion characterization of NiO thin films prepared by nebulized spray technique"*** Int.J. ChemTech Res., **6**(13):5196-5202, (2014).

[30] A. F. Saleh, ***" Structural and morphological studies of NiO thin films prepared by Rapid thermal oxidation method"*** International Journal of Application or Innovation in Engineering & Management (IJAIEM), **2**(1) :(2013).

[31] P. M. S. Monk, S. P. Akhtar, J. Boutevin and J. R. Duffield, ***"Towardthe tailoring of electrochromic bands of metal – oxide mixtures",*** Electrochim. Acta **46:**2091-2096, (2001).

[32] P.M.S. Monk, R.J. Mortimer, D.R. Rosseinsky, *"**Electrochromism: Fundamentals and Applications**"* Weinheim, VCH, (1995).

[33] I. Hamberg, C.G. Granqvist, *"**Evaporated Sn-doped In_2O_3 films: Basic optical properties and applications to energy-efficient windows**"* J. Appl. Phys., 60(11): (1986).

[34] C.G. Granqvist, A. Hultåker,*" **Electrochromism and Electrochromic Devices**"* Thin Solid Films**411**,1(2002)**.**

[35] *http://www.econtrol-glas.de/* (Date accessed: 13 April 2010).

[36] C.G. Granqvist, "***Handbook of Inorganic Electrochromic Materials***" Amsterdam, Elsevier (1995).

[37] A. Al-Kahlout, *"**Electrochromic properties and coloration mechanisms of sol-gel NiO-TiO_2 layers and devices built with them***" Ph. D. Thesis, University of Saarland and Leibniz-Institutfu¨rNeueMaterialien- (INM) and University of Saarland,(2006).

[38] O. Glemser, J. Einerhand, "**Die struktur höherer nickelhydroxyde**" *Anorg. Allg. Chem.* **261**(1-2): 43-51, (1950).

[39] N. Sac-Epe, M.R. Palacin, A. Delahaye-Vidal, Y.Chabre, J-M. Tarascon*,*" ***Batteries for the 21st Century***" J. Electrochem.Soc., **145** (1998).

[40] P. Oliva, J. Lenoardi, J.F.Laurent, C.Delmas, J.J. Braconnier, M. Figlarz, F. Fievet, A. De Guibert, *"**Review of the structure and the electrochemistry of nickel hydroxides and oxy-hydroxides**"* Journal of Power Sources, **8**(2): 229-255, (1982).

[41] S. Deabate, F. Henn, ***"Structural modifications and electrochemical behavior of the β(II)-Ni(OH)$_2$/β(III)-NiOOH redox couple upon galvanostatic charging/discharging cycling"*** ElectrochimicaActa, **50**(14): 2823-2835, (2005).

[42] H.Bode, K. Dehmelt and J. Witte, ***"Zurkenntnis der nickel hydroxid electrode —I.Über das nickel (II)-hydroxidhydrat"*** ElectrochimicaActa,**11**(8): 1079, (1966).

[43] R.S. Mcewen***, "Crystallographic studies on nickel hydroxide and the higher nickel oxides"*** J. Phys. Chem.,**75**(12):1782, (1971).

[44] S. Le, M. Figlarz***," Note sur l'article : "Zurkenntnis der Nickel-hydroxidelektrode—III. ThermogravimetrischeUntersuchungen a Nickel(II)-hydroxigen" par W. Dennstedt et W. Löser*** "ElectrochimicaActa, **18**(1):123, (1973).

[45] N. Sac-Epee, M.R. Palacin, B. Beaudoin, A. Delahaye-Vidal, T.Jamin, Y.Chabre, J-M. Tarascon***, " On the origin of the second low-voltage plateau in secondary alkaline batteries with nickel hydroxide positive electrodes"*** J. Electrochem. Soc., **144**(11): 3896-3907, (1997).

[46] R. Barnard, C. F. Randell and F. L. Tye," **Studies concerning charged nickel hydroxide electrodes: Part III. Reversible potentials at low states of charge"** *J. Electroanal. Chem.* 119 (1):17-24, (1981).

[47] R. Barnard, G. T. Crickmore, J. A. Lee, F. L. Tye,**" The cause of residual capacity in nickel oxyhydroxide electrodes"**, J. *Appl. Electrochem.* **10**(1): 61-70, (1980).

[48] I.Bouessay, A. Rougier, P. Poizot, J. Moscovici, A. Michalowicz, J.-M.Tarascon, ***"Electrochromic degradation in nickel oxide thin film: A self-discharge and dissolution phenomenon"*** ElectrochimicaActa, **50**(18): 3737-3745,(2005).

[49] M. C. Fantini, C. R. C. Carvalho ; A, Gorenstein, ***"Electrochromic properties and temperature dependence of chemically deposited Ni(OH)x thin film"*** SPIE Proceedings, **1536** 81, (1991).

[50] J. Y. Park, K. S. Ahn, Y. C Nah, H. S. Shim***," Electrochemical and electrochromic properties of Ni oxide thin films prepared by a sol–gel method"*** Journal of Sol-Gel Science and Technology, **31**(1): 323-328, (2004).

[51] A. Azens, L. Kullman, G. Vaivars, H. Nordborg and C.G. Granqvist, ***"Sputter-deposited nickel oxide for electrochromic applications"*** Solid State Ionics, 113-115:449-456, (1998).

[52] D.D. Ragan, P. Svedlindh, C.G. Granqvist, ***"Electrochromic Ni oxide films studied by magnetic measurements"*** Solar Energy Mterials& Solar Cells, **54** 247, (1998).

[53] J.S.E.M. Svensson, C.G. Granqvist, ***"Electrochromic hydrated nickel oxide coatings for energy efficient windows: Optical properties and coloration mechanism"*** Appl Phys Lett**, 49:**1566-1568, (1986)**.**

[54] L. Ottaviano, A. Pennis, F. Simone, ***"Electrochromic nickel oxidefilms made by reactive r.f. sputtering from different targets"*** Surfaceand Interface Analysis, **36** 1335, (2004).

[55] K. Yoshimura, T. Miki, S. Tanemura**,** ***"Direct observation of the structure of nickel oxide electrochromic thin films by HRTEM"*** Optical Materials Technology for Energy Efficiency and Solar EnergyConversion, Thursday 13 July 1995, San Diego, CA, USA, SPIEProceedings, **127** 2531, (1995)**.**

[56] I. Saadeddin, ***"Preperation and characterization of new transparent conducting oxides based on SnO_2 and In_2O_3: ceramics and thin films"*** PhD. thesis, Bordeaux I University, Bordeaux, France, (2007).

[57] T. Seike, J. Nagai, ***"Electrochromism of 3d transition metal oxides"*** Solar Energy Materials, **22**(2-3):107-117, (1991).

[58] D. B. Chrisey and G. K. Hubler, ***"Plused laser deposition of thin films"*** John Wiley and Sons, New York (1994).

[59] *http://en.wikipedia.org/wiki/Pulsed_laser_deposition* (Date accessed:13 April 2010).

[60] H.S.Hilal, R.M.A.Ismail, A.El-Hamouz, A.Zyoud, I.Saadeddin, ***"Effect of cooling rate of pre-annealedCds thin film electrodes prepared by chemical bath deposition inhancement of photo-electrochemical characteristics"*** elecrochimActa**, 54,** 3433-3440 (2009).

[61] http://en.wikipedia.org/wiki/Dip-coating (Date accessed: 13 April2010).

[62] M.N. Rahaman, *"Ceramic processing. bocaraton*: *CRC press*" **ISBN 0-8493-7285-2***"* Taylor &Francis 242 – 244, (2007).

[63] L. D. Landau and B. G. Levich, "***Entrainment of fluid by the drivenPlate****"* Acta Phys chem**, 17,** 42 (1942).

[64] L. L. Hench and J. K. West**,** ***"The sol-gel process"*** Chem. Rev., **90**(1): 33-72, (1990).

[65] G. Sasikala, R. Dhanasekaran, C. Subramanian, ***"Electrodeposition & Optical Characterization of Cds thin films on ITO/coated glass"***Thin Solid Film**, 302,** 71-76 (1997).

[66] Milton Ohring, **"The Materials Science of Thin Films"**, Boston: Academic Press, California, USA, P.197, (1992).

[67] William R. Birch, **"Coating: an introduction to the cleaning procedure",** June 2000.

[68] William Andrew, **"Hand book of thin film deposition processes and techniques"** 2nd edition, 2001.

[69] Guo-rui Fu, Zhong-ai Hu*, Li-jing Xie, Xiao-qing Jin, Yu-long Xie,Yao-xian Wang, Zi-yu Zhang,Yu-ying Yang, Hong-ying Wu, "**Electrodeposition of nickel hydroxide films on nickel foil and its electrochemical performances for supercapacitor"** *Int. J. Electrochem. Sci.,* 4:1052 – 1062**, (2009).**

[70] Thierry Pauporte´z, "**A simplified method for WO3 electrodeposition"** *Journal of The Electrochemical Society*, **149 (**11): C539-C545, (2002).

[71] W.L. Kwong, H. Qiu, A. Nakaruk, P. Koshy, and C.C. Sorrell*, "**Photoelectrochemical Properties of WO3 Thin Films Prepared by Electrodeposition**" Energy Procedia, 34: 617 – 626, (2013).

[72] S. Ferro, C.A. Martinez-Huitle, A. De Battisti, " **Electroxidation of oxalic acid at different electrode materials**" J. Appl. Electrochem.40, 1779 (2010).

[73] Dalavi and S Dhanaji, "**Synthesis and characterization of nanostructured NiO thin films and their electrochromic properties**" thesis, Shivaji University, (2012).

[74] T. S. Kayed, A. F. Qasrawi, and Khaled A. Elsayed, ***"Optical characterization of the MgO/InSe interface",*** Phys. Status Solid B, **252**(3): 621–625, (2015).

[75] Saturi Baco[1, *], Abdullah Chik[2], Fouziah Md. Yassin[1], ***"Study on optical properties of tin oxide thin film at different annealing temperatyre"***, Journal of Science and Technology, **4**(1): (2012).

[76] R. K. Jamal, Q. G. Al-Zaidi, N. M. Saeed, I. N. Taaban, ***"Preparation and characterization of nickel oxide thin films by electrostatic spray technique"*** Iraqi Journal of Science, **57**(1):618-623, (2016).

[77] S. A. Mahmoud, S. Alshomer, M. A. Tarawnh,***"Structural and optical dispersion characterisation of sprayed nickel oxide thin films"*** Journal of Modern Physics, 2, 1178-1186 (2011).

[78] F. Wooten, ***"Optical properties of solids"*** Academic, New York, (1981).

[79] R. A. Smith, ***"Semiconductors"***Cambridge University Press, Cambridge, (1978).

[80] J. C. Manifacier, M. De Murcia, I. Fillard, E. Vicario, ***"Optical andelectrical properties of SnO_2 thin films in relation to their stoichiometric deviation and their crystalline structure"*** Thin SolidFilms, **41** 127, (1977).

[81] S.B. Kulkarni, V.S. Jamadade, D.S. Dhawale, C.D. Lokhande, ***"Synthesis and characterization of [beta]-$Ni(OH)_2$ up grown nanoflaskes by SILAR method"***Appl Surf Sci, **255**: 8390, (2009).

[82] Hong-Ying Wu* and Huan-Wen Wang, " **Electrochemical synthesis of nickel oxide nanoparticulate films on nickel foils for high-performance electrode materials of supercapacitors"** Int. J. Electrochem. Sci., 7: 4405 – 4417, (2012).

[83] K.K. Purushothaman, G. Muralidharan, **"The effect of annealing temperature on the electrochromic properties of nanostructured NiO films"** Solar EnergyMaterials&SolarCells, 93:1195–1201, (2009).

[84] Evan L. Runnerstrom,[ab] Anna Llorde´s,[a] Sebastien D. Lounisac and Delia J. Milliron[*ad]**, "Nanostructured electrochromic smart windows: traditional materials and NIR-selective plasmonic nanocrystals"** *Chem. Commun.*, **50**:10555—10572, (2014).

[85] Kwo-Hsiung Young [1,2,*], Lixin Wang [2] , Shuli Yan [1] , Xingqun Liao [3,4], Tiejun Meng [2] , Haoting Shen [2] and William C. Mays [2], "

Fabrications of high-capacity alpha-$Ni(OH)_2$" *Batteries,* **3**(1): 6, (2017).

[86] Yudong Zhao,[a] Gaochen Gu,[b] Shengquan You,[a] Renhua Ji,[c] Hui Suo,*[a] Chun Zhao*[a] and Fengmin Liu[a] " **Preparation of $Ni(OH)_2$ nanosheets on Ni foam *via* a direct precipitation method for a highly sensitive non-enzymatic glucose sensor"** RSC Adv, **5**(66): 53665-53670, (2015).

جامعة النجاح الوطنية

كلية الدراسات العليا

خصائص التلوين الكهربائي لطبقات أكسيد النيكل (NiO) الرقيقة المحضرة بطريقة الترسيب الكهربائي : تحديد العوامل المثلى للتحضير

إعداد

مصطفى نعيم حسين واكد

إشراف

د .إياد سعد الدين

د .محمد سليمان إشتية

قدمت هذه الرسالة استكمالاً لمتطلبات الحصول على درجة الماجستير في الفيزياء بكلية الدراسات العليا في جامعة النجاح الوطنية في نابلس، فلسطين.

2017

خصائص التلوين الكهربائي لطبقات أكسيد النيكل (NiO) الرقيقة المحضرة بطريقة الترسيب الكهربائي : تحديد العوامل المثلى للتحضير

إعداد

مصطفى نعيم حسين واكد

إشراف

د . إياد سعد الدين

د . محمد سليمان

الملخص

تم تحضير أفلام NiO الرقيقة النانوية على شرائح من الزجاج الموصل (FTO/glass) بطريقة الترسيب الكهربائي. من اجل تلك الافلام تم عمل دراسة مقارنة لتأثير طرق تنظيف مختلفة وفولتيات متعددة للترسيب وتراكيز مولارية مختلفة على الالتصاق والتجانس و خصائص التلوين الكهربائي والبصرية والتركيبية.

خصائص الالتصاق والتجانس تم دراستها باستعمال مجهر ذو قوة تكبير (100x, 400x). خصائص التلوين الكهربائي (فعالية التلوين والثبات وزمن التبديل والمعكوسية) تم تحديدها باستعمال اقتران الفولتية (CV) و (CA) و النفاذية خلال (CA).

طيف النفاذية في مدى 200 الى 1000 نانوميتر استعمل ايضا لتحديد بعض العوامل البصرية (النفاذية وسمك الفلم وفجوة الطاقة). أفضل خصائص التصاق وتجانس للافلام لوحظت عند معالجة الشرائح باستخدام طريقة التنظيف السادسة.

أفضل خصائص تلوين كهربائية وبصرية حصل عليها عند تحضير الافلام عند فولتية -700 ملي فولت وتركيز مولاري 1 مولارتي.